LA-2405

LOS ALAMOS SCIENTIFIC LABORATORY
OF THE UNIVERSITY OF CALIFORNIA o LOS ALAMOS NEW MEXICO

SOME SEISMIC EFFECTS OF UNDERGROUND EXPLOSIONS IN CAVITIES

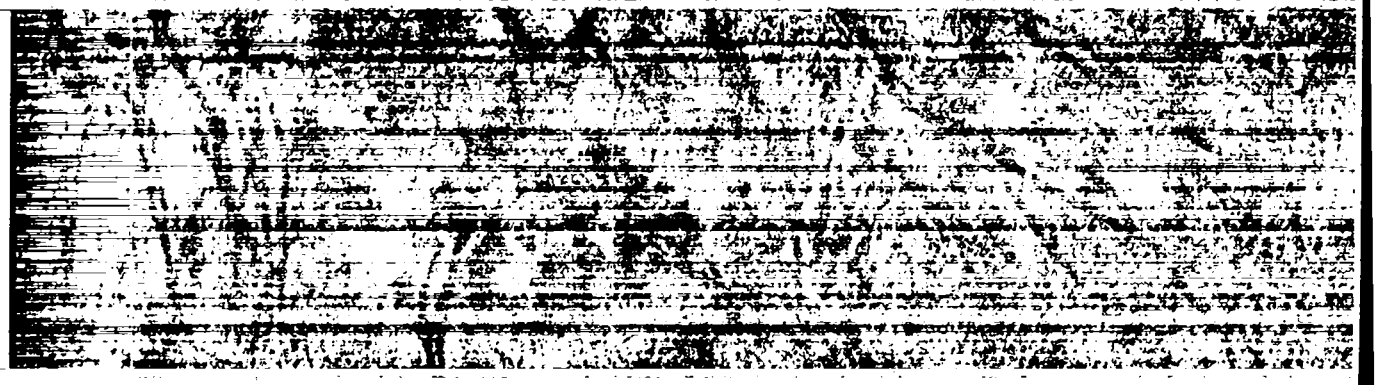

Printed in USA. Price $1.25. Available from the

Office of Technical Services
U. S. Department of Commerce
Washington 25, D. C.

LA-2405
NUCLEAR EXPLOSIONS--PEACEFUL
APPLICATIONS
TID-4500 (15th Ed.)

LOS ALAMOS SCIENTIFIC LABORATORY
OF THE UNIVERSITY OF CALIFORNIA LOS ALAMOS NEW MEXICO

REPORT WRITTEN: February 29, 1960

REPORT DISTRIBUTED: November 15, 1960

SOME SEISMIC EFFECTS OF UNDERGROUND EXPLOSIONS IN CAVITIES

by

George L. Lamb, Jr.

Contract W-7405-ENG. 36 with the U. S. Atomic Energy Commission

ABSTRACT

The concealment of nuclear explosions by containing them within underground cavities of a size sufficient to ensure the elastic behavior of the side walls has been suggested. In the present report, a number of effects created by the seismic signal radiated by an explosion in such a cavity are investigated theoretically. The first chapter contains a résumé of a standard calculation of the Rayleigh waves generated by a source of compressional waves in a semi-infinite homogeneous elastic medium. The second chapter is concerned with the stress concentration around a spherical cavity excised from a homogeneous elastic medium acted on by an arbitrary body force. The results are then specialized to the case of a uniform gravitational field with vanishing lateral displacement. The third chapter considers the stress distribution around a prolate spheroidal cavity in a uniform gravitational field with vanishing lateral displacement. The fourth chapter contains a discussion of the plastic expansion of a spherical cavity in an infinite elastic medium. Finally, the fifth chapter discusses the seismic waves generated by an air burst.

ACKNOWLEDGMENTS

The author wishes to express his thanks to Prof. H. A. Bethe for outlining the program of research on the detection problem, for his many suggestions and comments and for general inspiration. He is also indebted to Dr. James E. Young (T-DO) for a number of useful conversations and to Mr. L. W. Mann (T-5) for carrying out the machine computation involved in Chapter 3.

CONTENTS

Figures

CHAPTER 1

RAYLEIGH WAVES GENERATED BY AN EXPLOSION IN A CAVITY EXCISED FROM A HOMOGENEOUS ELASTIC HALF-SPACE

1.1 Introduction

Various aspects of wave propagation in a homogeneous elastic half-space have been considered for many years.[1] In the present treatment, the seismic Rayleigh wave due to a blast contained within a spherical cavity excised from a homogeneous elastic half-space is calculated. The results are used to estimate the detectability of nuclear explosions confined within such a cavity. Assuming that the cavity is of a size sufficient to ensure the elastic behavior of the walls (and this is the essence of the proposal to employ this means of containment), the theory of linear elasticity may be applied. Furthermore, only the low frequency waves with periods in the range from 10 to 50 sec are of interest. Since the corresponding wavelengths are much larger than the size of the cavity, the source may be represented as a point source of appropriate strength. Although this simplification reduces a large portion of the problem to a type which has been analyzed extensively, the solution is presented here in full in order to exhibit the method to be used in other similar but more complicated problems contemplated for the future.

1.2 Mathematical Formulation of the Problem

It is required to solve the vector wave equation

$$\rho \frac{\partial^2 \vec{s}}{\partial t^2} = (\lambda + 2\mu)\nabla(\nabla \cdot \vec{s}) - \mu \nabla x \nabla x \vec{s} + \vec{\Omega}(\vec{r}, t) \tag{1.1}$$

where

$\vec{\Omega}(\vec{r}, t) = \nabla Q_0 \delta(\vec{r} - \vec{r}_0) e^{-i\omega t}$ = the source function for harmonic compressional waves

$\vec{s}(\vec{r}, t)$ = elastic displacement

ρ = density of the elastic medium

λ, μ = Lamé constants

It is convenient to decompose the displacement $\vec{s}(\vec{r}, t)$ into compressional and shear components. In the present problem having cylindrical symmetry, this may be accomplished by introducing two scalar potentials φ and ψ according to the definition

$$\vec{s}(\vec{r}, t) = \nabla\varphi - \nabla x \nabla x \vec{k}\psi \tag{1.2}$$

where $\vec{k}$ is a unit vector along the vertical Z axis (see Fig. 1). Extracting a sinusoidal time dependence $e^{-i\omega t}$, and introducing the compressional and shear phase velocities c_L and c_T, respectively, by $c_L^2 = (\lambda + 2\mu)/\rho$ and $c_T^2 = \mu/\rho$, one obtains two scalar wave equations of the form

$$\begin{aligned} \nabla^2\varphi + k_L^2\varphi &= -q_0 \delta(\vec{r} - \vec{r}_0) \\ \nabla^2\psi + k_T^2\psi &= 0 \end{aligned} \tag{1.3}$$

where $k_L = \omega/c_L$, $k_T = \omega/c_T$ and $q_0 = Q_0/\rho c_L^2$

Introducing longitudinal and transverse Green's functions G_L and G_T, respectively, which have vanishing normal derivatives on the boundary $z = 0$,

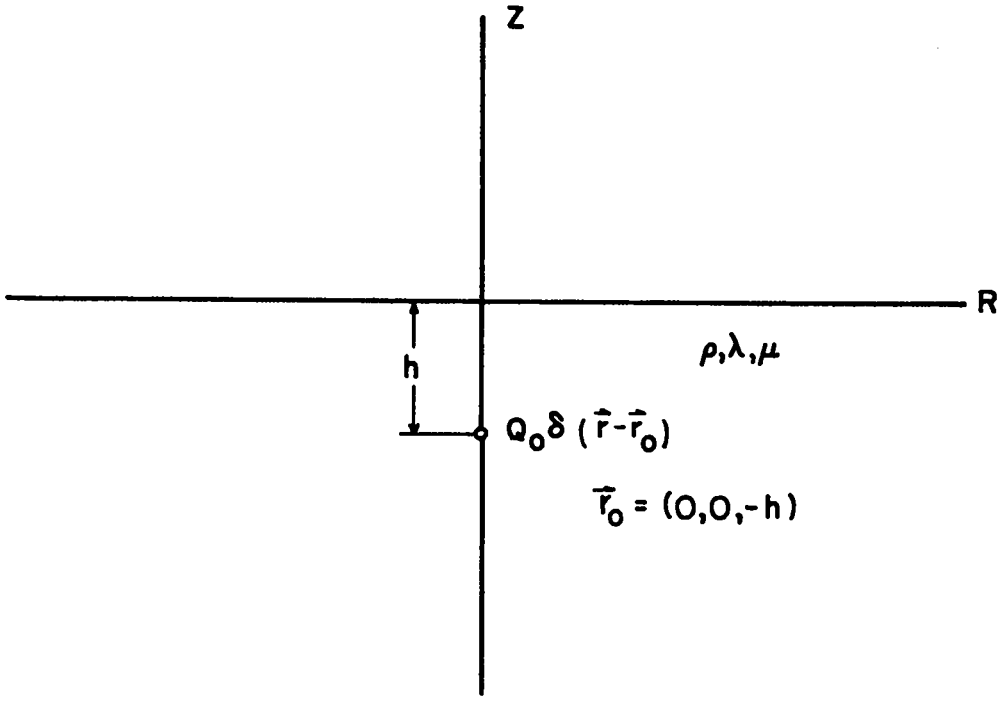

Fig. 1 Coordinate system for Rayleigh wave calculation.

Eqs. (1.3) may be converted into a pair of integral equations. Since it proves more convenient to deal with $\partial_r \varphi \equiv \partial\varphi/\partial r$ rather than with φ itself, the equations

$$\begin{aligned} \partial_r \varphi &= q_0 \partial_r G_L(\vec{r}/\vec{r}_0) + \int ds' G_L(\vec{r}/\vec{r}') \partial^2_{z'r'} \varphi \\ \psi &= \int ds' G_T(\vec{r}/\vec{r}') \partial_{z'} \psi \end{aligned} \tag{1.4}$$

are obtained by means of Green's theorem. The functions G_L and G_T are given by

$$G_{L,T} = \frac{1}{4\pi}\left(\frac{e^{ik_{L,T}R}}{R} + \frac{e^{ik_{L,T}R'}}{R'}\right), \quad R^2 = (r-r')^2 + (z-z')^2,$$
$$R'^2 = (r-r')^2 + (z+z')^2 \tag{1.5}$$

The vanishing of normal and tangential stresses at the surface of the elastic half-space gives rise to the boundary conditions

$$\begin{aligned} \tau_{zr} &= \mu\left(\frac{\partial s_r}{\partial z} + \frac{\partial s_z}{\partial r}\right) = 0 \\ \tau_{zz} &= \lambda \nabla \cdot \vec{s} + 2\mu \frac{\partial s_z}{\partial z} = 0 \end{aligned} \tag{1.6}$$

where, from Eq. (1.2)

$$\begin{aligned} s_r &= \frac{\partial \varphi}{\partial r} + \frac{\partial^2 \psi}{\partial z \partial r} \\ s_z &= \frac{\partial \varphi}{\partial z} + k_T^2 \psi + \frac{\partial^2 \psi}{\partial z^2} \end{aligned} \tag{1.7}$$

Incorporation of the boundary conditions into Eqs. (1.4) results in the following pair of coupled integral equations.

$$\partial_r \varphi = q_0 \partial_r G_L(\vec{r}/\vec{r}_0) - \int ds' G_L\left(\frac{1}{2}k_T^2 \partial_{r'}\psi + \partial^3_{r'z'z'}\psi\right)$$
$$\psi = \int ds' G_T\left[\frac{\lambda}{2\mu}\frac{k_L^2}{k_T^2}\varphi - \frac{1}{k_T^2}\left(\partial^2_{z'z'}\varphi + \partial^3_{z'z'z'}\psi\right)\right] \tag{1.8}$$

Since the problem possesses cylindrical symmetry about the Z axis, the solution may be expressed in terms of Fourier-Bessel transforms. Hence, introducing the integral representations

$$\varphi = \varphi^{(0)} + \varphi^{(0)}_{\text{image}} + \int_0^\infty \kappa d\kappa \Phi(\kappa) J_0(\kappa r) e^{-i\zeta_L z}$$
$$\psi = \int_0^\infty \kappa d\kappa \Psi(\kappa) J_0(\kappa r) e^{-i\zeta_T z} \tag{1.9}$$

where $\varphi^{(0)} + \varphi^{(0)}_{\text{image}}$, the potential for the source plus its image, is given by

$$\varphi^{(0)} + \varphi^{(0)}_{\text{image}} = q_0 G_L(\vec{r}/0, -h)$$

and $\zeta_L^2 = k_L^2 - \kappa^2$, $\zeta_T^2 = k_T^2 - \kappa^2$, one can reduce Eqs. (1.8) to the following pair of algebraic equations

$$2\zeta_L \Phi + i\left(k_T^2 - 2\zeta_T^2\right)\Psi = 0$$
$$\left(\frac{\lambda}{2\mu}k_L^2 + \zeta_L^2\right)\Phi + i\zeta_T \kappa^2 \Psi = \frac{q_0}{2\pi}\left(\frac{\lambda}{2\mu}k_L^2 + \zeta_L^2\right)\frac{e^{i\zeta_L h}}{i\zeta_L} \tag{1.10}$$

Confining attention to the case $\lambda = \mu$ (Poisson's ratio = 1/4) so that $k_T^2 = 3k_L^2$, solving Eqs. (1.10) for Φ and Ψ and substituting the resulting expressions into Eqs. (1.9), one finds

$$\varphi = \frac{q_0}{4\pi}\left[\frac{e^{ik_L R}}{R} + \frac{e^{ik_L R'}}{R'} + \frac{2}{i}\int_0^\infty \kappa d\kappa J_0(\kappa r) e^{-i\zeta_L(z+h)} \frac{\left(k_T^2 - 2\kappa^2\right)^2}{\zeta_L F(\kappa)}\right]$$

$$\psi = -\frac{q_0}{4\pi} 4 \int_0^\infty \kappa d\kappa J_0(\kappa r) e^{-i\zeta_T z - i\zeta_L h} \frac{\left(k_T^2 - 2\kappa^2\right)}{F(\kappa)} \tag{1.11}$$

where

$$F(\kappa) \equiv \left(k_T^2 - 2\kappa^2\right)^2 + 4\kappa^2 \zeta_L \zeta_T \tag{1.12}$$

Employing the second of Eqs. (1.7), the vertical displacement at the surface of the half-space $z = 0$ is found to be

$$s_z(r, 0) = \frac{q_0}{2\pi} \int_0^\infty \kappa d\kappa J_0(\kappa r) e^{-i\zeta_L h} \frac{k_T^2\left(2\kappa^2 - k_T^2\right)}{F(\kappa)} \tag{1.13}$$

1.3 Determination of the Rayleigh Wave

The total displacement at any point in the solid more than a few wavelengths from the source can be thought of as being composed of two parts. One of these, a disturbance which falls off exponentially with depth beneath the surface, but only as $r^{-1/2}$ with radial distance away from the source, is the Rayleigh surface wave. The other, the body wave, falls off in all directions inversely with distance from the source. Hence, at large distances, the disturbance at the surface will be due primarily to the surface wave. Since this is the region of interest for seismic detection, only the disturbance due to the surface wave need be considered.

The above-mentioned decomposition of the total displacement has a natural mathematical counterpart when the integral in Eq. (1.13) is evaluated by means of the Cauchy integral theorem. Such an evaluation in terms of an

equivalent integral in a complex κ plane gives rise to two contributions, one from a pole at $\kappa = 1.09k_T$ and the other from two branch cuts. The contribution from the pole corresponds to the surface wave, and the contribution from the branch cuts corresponds to the body wave. Since only the surface wave is being considered, the branch cuts will be ignored. Application of the Cauchy integral theorems then yields

$$s_z(r, 0) = 2\pi i \frac{q_0}{4\pi} \left[\frac{\kappa H_0^{(1)}(\kappa r) e^{-i\zeta_L h} k_T^2 \left(2\kappa^2 - k_T^2\right)}{\frac{\partial F}{\partial \kappa}} \right]_{\kappa = 1.09k_T} \tag{1.14}$$

Carrying out the indicated operations, employing the asymptotic representation for the Hankel function, and setting $1.09k_T \equiv k_R$, the propagation constant for Rayleigh waves,

$$s_z(r, 0) = -0.1 \frac{q_0}{c_R^{3/2} r^{1/2}} \omega^{3/2} e^{-0.84k_R h} e^{-i(\omega t^* - \pi/4)}$$

$$\equiv q_0 A(\omega, r) e^{-i(\omega t^* - \pi/4)} \tag{1.15}$$

where $t^* \equiv t - r/c_R$

Eq. (1.15) represents the Rayleigh surface wave due to a point source in an elastic half-space.

1.4 Solution for Step-Function Pressure

A solution to the actual problem under consideration remains to be constructed from the above result, namely, a step-function pressure applied to the inside of a spherical cavity.

The sinusoidal excitation of the cavity will first be considered, and then the result for a step-function excitation will be synthesized from this. Since

in the vicinity of the cavity the motion should be radial, one may assume a spherically symmetric displacement potential and write

$$\varphi^{(0)} = \frac{q_0}{4\pi} \frac{e^{ikR}}{R} \tag{1.16}$$

The radial displacement is then given by

$$s_R = \frac{\partial \varphi^{(0)}}{\partial R} \simeq -\frac{q_0}{4\pi R^2} e^{ikR}, \quad R \ll \lambda \tag{1.17}$$

On the surface of the spherical cavity of radius a,

$$\sigma_R\Big|_{R=a} = -p_0 = (\lambda + 2\mu) \frac{\partial s^{(0)}}{\partial R}\Big|_{R=a} + 2\lambda \frac{s^{(0)}}{R}\Big|_{R=a} = \frac{\mu q_0}{\pi a^3} e^{ikR} \tag{1.18}$$

The pressure p_0 is assumed to be related to the energy E of the gas by the relation $p_0 = E\,(\gamma - 1)/V$. Assuming a uniform distribution of the energy of an explosion throughout a cavity of radius a

$$p_0 = \frac{(\gamma - 1)E}{\frac{4\pi}{3} a^3} \tag{1.19}$$

Equating Eqs. (1.18) and (1.19), the equivalent source strength is found to be

$$\frac{q_0}{4\pi} = -\frac{3(\gamma - 1)E}{16\pi\mu} \tag{1.20}$$

The step-function pressure applied to the cavity wall may be written in terms of its Fourier spectrum according to the relations

$$p(t) = \left\{ \begin{array}{l} P_0, t \geq 0 \\ \\ 0, t < 0 \end{array} \right\} = \frac{P_0}{\pi} \int_0^\infty \frac{d\omega}{\omega} \sin\omega t = -\mathrm{Im} \frac{P_0}{2\pi} \int_{-\infty}^\infty \frac{d\omega}{\omega} e^{-i\omega t} \tag{1.21}$$

Employing this same prescription to synthesize the displacement corresponding to this source term,

$$s_z(r, 0) = -\mathrm{Im} \int_{-\infty}^{\infty} \hat{q}(\omega) A(\omega, r) e^{-i(\omega t^* - \pi/4)} \tag{1.22}$$

From Eqs. (1.18) and (1.21)

$$\hat{p}(\omega) = \frac{P_0}{\pi\omega} = -\frac{\mu}{\pi a^3} \hat{q}(\omega) \tag{1.23}$$

Eq. (1.22) may now be written

$$s_z(r, 0) = -\frac{3(\gamma - 1)E}{20\pi\mu c_R^{3/2}} \frac{1}{\sqrt{r}} \int_0^{\infty} d\omega \omega^{1/2} e^{-0.84 k_R h} \sin\left(\omega t^* - \frac{\pi}{4}\right) \tag{1.24}$$

In order to simulate the attenuation of higher frequencies, an attenuation factor $e^{-\alpha\omega}$ is introduced into the integrand of Eq. (1.24). Performing the integration[2] one finds

$$s_z(r, 0) = \frac{3(\gamma - 1)E}{40\sqrt{\pi}\mu c_R^{3/2}\sqrt{r}} \frac{\sin\left(\frac{\pi}{4} - \frac{3}{2}\tan^{-1} p\right)}{(a + \alpha)^{3/2}\left(1 + p^2\right)^{3/4}} \tag{1.25}$$

where $p \equiv t^*/(a + \alpha)$ with $a \equiv 0.84h/c_R$. Frequency components with periods shorter than 10 sec will be attenuated by at least e^{-1} with respect to those of zero frequency by setting $\alpha = 10/2\pi = 1.59$ sec. Assuming a burial depth $h = 1$ km and employing the value $c_R = 3.2$ km/sec, one finds $a = 0.26$ sec.

The shape of the wave predicted by Eq. (1.25) is shown in Fig. 2. The maximum value of the time dependent term $\sin\left(\frac{\pi}{4} - \frac{3}{2}\tan^{-1} p\right)/\left(1 + p^2\right)^{3/4}$ is seen from Fig. 2 to be approximately 0.9. Employing the values $\gamma = 1.2$, $\mu = 20$ kb, the maximum value of $s_z(r, 0)$ is found to be

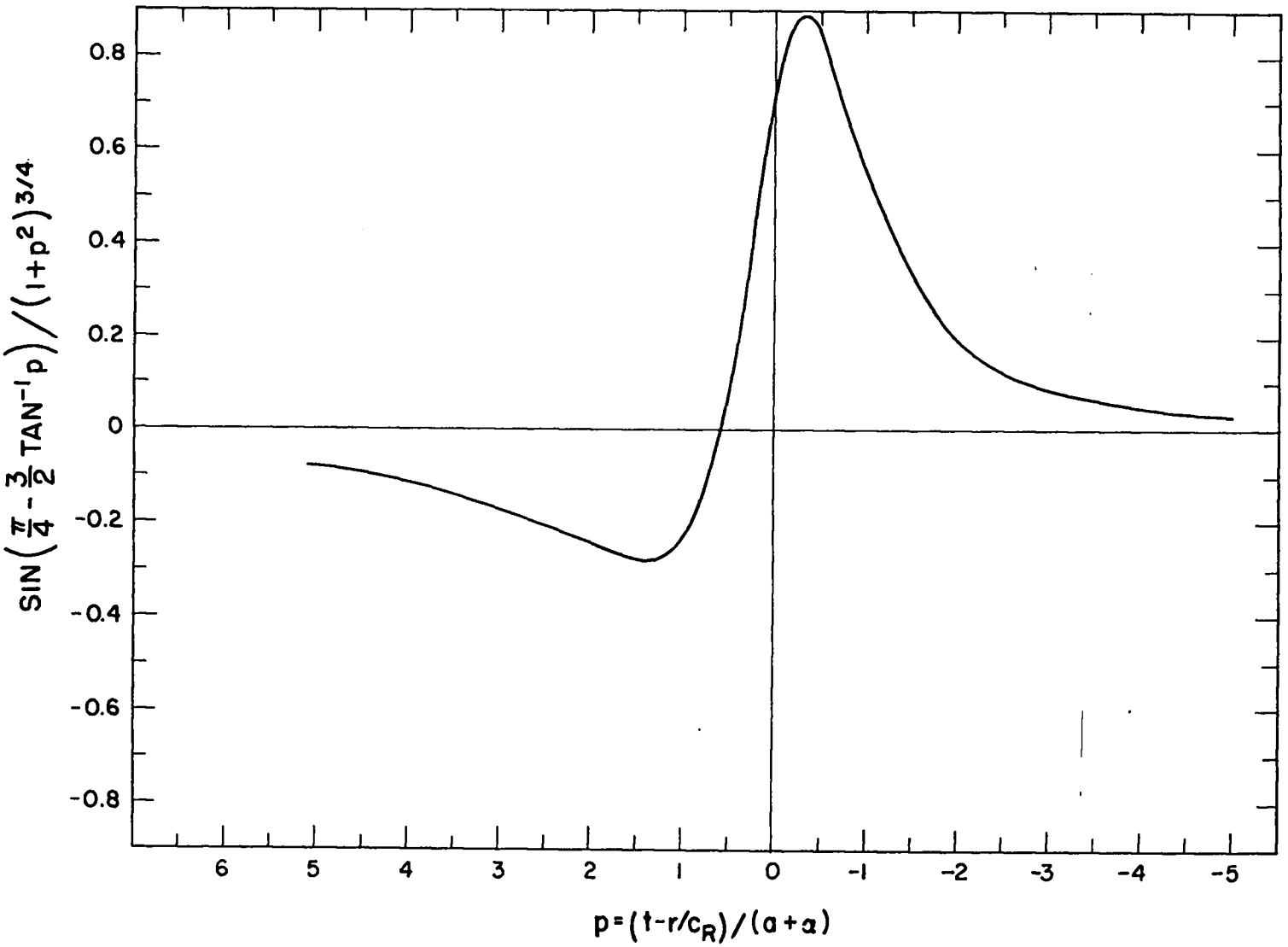

Fig. 2 Shape of Rayleigh wave due to step function pressure on cavity wall.

$$s_z(r,0)\Big|_{max} = 1.1\frac{E}{\sqrt{r}} \tag{1.26}$$

where E is in kt, r in km and s_z in microns. This result predicts a maximum displacement of 0.35 micron at a distance of 1000 km from a 10 kt explosion.

From Fig. 2 it is seen that the main disturbance is a single pulse. The predominant period of this pulse is obtained by finding the maximum in the spectrum function $\omega^{1/2}e^{-0.84\omega h/c_R}$ of Eq. (1.24). Setting h = 1 km and c_R = 3.2 km/sec, one finds

$$T \simeq 3.5 \text{ sec}$$

Although displacement amplitudes predicted on the basis of the present simple theory are not unreasonable, an essential feature of seismograms is noticeably absent, namely, a periodic disturbance containing a number of wavelengths.

One can, of course, look at the amplitudes per unit frequency in the above result by integrating Eq. (1.22) over a small frequency interval $\Delta\omega$ about a central frequency ω_0. Employing the complex counterpart of Eq. (1.22),

$$s_z(r,0) = \int_{\omega_0-\Delta\omega/2}^{\omega_0+\Delta\omega/2} d\omega \hat{q}(\omega)A(\omega_0, r)e^{-i(\omega t^*-\pi/4)}$$

$$= \frac{3(\gamma-1)E\omega_0^{3/2}}{40\pi\mu\sqrt{r}\, c_R^{3/2}}\left(\frac{\Delta\omega}{\omega_0}\right)\frac{\sin\tau\Delta\omega/2}{\tau\Delta\omega/2}e^{-i\left(\omega_0 t_1-\pi/4\right)}e^{-0.84\omega_0 h/c_R} \tag{1.27}$$

The displacement per unit frequency is

$$\frac{s_z(r,0)}{\Delta\nu} = \frac{3(\gamma-1)E}{20\mu\, c_R^{3/2}}\frac{\sqrt{\omega_0}}{\sqrt{r}}e^{-0.84h\omega_0/c_R}\left(\frac{\sin\tau\Delta\omega/2}{\tau\Delta\omega/2}\right)e^{-i\,\omega_0 t_1-\pi/4} \tag{1.28}$$

where

$$t_1 = t - r/c_R$$

$$\tau = t - r/U$$

with $U = d\omega/dk$, the group velocity. The maximum value of the expression in Eq. (1.28) is obtained for $\tau = 0$. Again setting $\gamma = 1.2$ and $\mu = 20$ kb and considering waves of 20 sec period,

$$\frac{s_z(\max)}{\Delta\nu} = 37\frac{E}{\sqrt{r}} \tag{1.29}$$

where s_z is in microns, E in kt and r in km. For a 10 kt explosion at 1000 km and a bandwidth $\Delta\nu = \nu/10 = 5 \times 10^{-3}$/sec,

$$s_z(\max) = 58 \text{ millimicrons} \tag{1.30}$$

Such an amplitude is detectable with present-day seismographs, but is below known noise levels.

It should be emphasized that this last calculation is particularly elementary. In particular, the frequency dependence indicates an increase with increasing frequency, while in the 20 sec range, the opposite is known to be true. A phenomenological attenuation coefficient could be introduced to simulate this effect, but the approximate nature of the calculation does not seem to warrant it.

CHAPTER 2

THE STRESS DISTRIBUTION AROUND A SPHERICAL CAVITY

2.1 Introduction

In employing an underground cavity to confine an explosion, it is considered essential that the walls behave elastically. Therefore the pressure within the cavity must not be large enough to cause cracks to open or the walls to deform plastically. It is known that rock can withstand considerable compressive stress but little tensile stress. Consequently the confinement of the explosion will be due almost entirely to the lithostatic pressure holding the wall in compression and forming a "hoop stress." The actual confining stress of a cavity at a depth h may be roughly equal to the lithostatic pressure ρgh but can depend to quite an extent upon the inhomogeneities in the stress field. In the present chapter, the stresses around a spherical cavity excised from a region in which an arbitrary stress distribution is initially present are calculated. It is shown that the effect of the initial stress field may be enough to cause the hoop stress acting on the cavity wall to vanish or even become tensile.[3]

2.2 Solution for an Arbitrary Stress Distribution

Assuming that prior to construction of the cavity the material is in a state of stress $\left(\sigma_x, \sigma_y, \sigma_z\right)$ with corresponding $\left(\epsilon_x, \epsilon_y, \epsilon_z\right)$, the displacement

potential $\phi^{(0)}$ defined by

$$\phi^{(0)} = \frac{1}{2}\left(\epsilon_x x^2 + \epsilon_y y^2 + \epsilon_z z^2\right) \tag{2.1}$$

may be introduced. Upon construction of the cavity, a new stress system will establish itself such that the normal and tangential components of stress on the cavity wall will vanish. This may be viewed mathematically as the addition of stresses compatible with the equations of elasticity which cancel at the cavity wall the stresses obtained from Eq. (2.1).

Such additional stresses are obtained from appropriate solutions of the basic equation of static elasticity.

$$(\lambda+\mu)\nabla(\nabla\cdot\hat{s}) + \mu\nabla^2\hat{s} = 0 \tag{2.2}$$

Expressing Eq. (2.1) in terms of a spherical coordinate system with origin at the center of the cavity, and with polar angle measured from the Z axis as usual,

$$\phi^{(0)} = a_{00}r^2 + r^2 \sum_{m=0}^{2} a_{2m} Y_{2m}(\theta, \varphi) \tag{2.3}$$

where Y_{2m} are the even spherical harmonics $P_2^m(\cos\theta)\cos m\varphi$. For convenience this will be considered as the real part of $P_2^m(\cos\theta)e^{im\varphi}$. The a_{mn}'s are given by

$$\begin{aligned} a_{00} &= \frac{1}{6}\nabla\cdot\hat{s} \\ a_{20} &= \frac{1}{4\mu}\left(\sigma_z + p_\ell\right) \\ a_{21} &= 0 \\ a_{22} &= \frac{1}{12\mu}\left(\sigma_x - \sigma_y\right) \end{aligned} \tag{2.4}$$

where $3p_{\ell} = -\left(\sigma_x + \sigma_y + \sigma_z\right)$

From the gradient of $\phi^{(0)}$ one may obtain the components of the displacement vector $\vec{s}^{(0)}$

$$
\begin{aligned}
s_r^{(0)} &= 2a_{00}r + 2r\Sigma a_{2m}Y_{2m} \\
s_\theta^{(0)} &= r\Sigma a_{2m}\frac{\partial Y_{2m}}{\partial\theta} \\
s_\varphi^{(0)} &= \frac{r}{\sin\theta}\Sigma m a_{2m}Y_{2m}
\end{aligned}
\tag{2.5}
$$

In spherical coordinates the relevant stresses are given in terms of the displacement by

$$
\begin{aligned}
\sigma_r &= \lambda\nabla\cdot\vec{s} + 2\mu\frac{\partial s_r}{\partial r} \\
\tau_{r\theta} &= \frac{\mu}{r}\left(\frac{\partial s_r}{\partial\theta} - s_\theta + r\frac{\partial s_\theta}{\partial r}\right) \\
\sigma_\theta &= \lambda\nabla\cdot\vec{s} + \frac{2\mu}{r}\left(\frac{\partial s_\theta}{\partial\theta} + s_r\right) \\
\sigma_\varphi &= \lambda\nabla\cdot\vec{s} + 2\mu\left(\frac{1}{r\sin\theta}\frac{\partial s_\varphi}{\partial\varphi} + \frac{s_r}{r} + \frac{s_\theta\cot\theta}{r}\right)
\end{aligned}
\tag{2.6}
$$

From the first two of Eqs. (2.6) one may obtain the normal and tangential components of stress on the cavity wall. Solutions of Eq. (2.2) are now required to cancel these stresses.

The solution of Eq. (2.2) may be expressed in terms of three scalar harmonic functions[4] ψ, χ and ω as follows:

$$
\begin{aligned}
\vec{s} &= \Sigma s_n \\
\vec{s}_n &= \nabla\psi_n + \nabla\times\left(\hat{a}_r\chi_n\right) + r^2\nabla\omega_n + \alpha_n r\omega_n
\end{aligned}
\tag{2.7}
$$

where n is an index specifying the positive or negative power of r in the given harmonic function and

$$\alpha_n = -2\frac{n\lambda + (3n+1)\mu}{(n+3)\lambda + (n+5)\mu} \tag{2.8}$$

Since solutions are required which vanish at large distances from the cavity, the index n is confined to negative integral values. Also, the purely shear solutions χ_n may be neglected. Therefore, the only admissible solutions are

$$\psi = \psi_{-1} + \psi_{-3} = A_{00}\frac{1}{r} + \frac{1}{r^3}\Sigma A_{2m} Y_{2m} \tag{2.9}$$

$$\omega = \omega_{-3} = \frac{1}{r^3}\Sigma B_{2m} Y_{2m} \tag{2.10}$$

These solutions give rise to corresponding displacements of the form

$$s^{(1)} = \nabla\psi = -\frac{A_{00}}{r}\vec{a}_r + \frac{1}{r^4}\Sigma A_{2m}\left(-3\vec{a}_r Y_{2m} + \vec{a}_\theta \frac{\partial Y_{2m}}{\partial\theta} - \vec{a}_\varphi \frac{im}{\sin\theta} Y_{2m}\right) \tag{2.11}$$

$$s^{(2)} = r^2\nabla\omega_{-3} + \alpha_{-3} r\omega_{-3}$$

$$= \frac{1}{r^2}\Sigma B_{2m}\left[\vec{a}_r\left(\alpha_{-3} - 3\right)Y_{2m} + \vec{a}_\theta \frac{\partial Y_{2m}}{\partial\theta} - \vec{a}_\varphi \frac{im}{\sin\theta} Y_{2m}\right] \tag{2.12}$$

From the boundary conditions $\sigma_r = \tau_{r\theta} = 0$ in the surface $r = a$ plus the fact that the spherical harmonics are linearly independent, one obtains the following set of three equations for the unknown amplitudes A_{00}, A_{2m} and B_{2m}:

$$0 = (6\lambda + 4\mu)a_{00} + \frac{4\mu A_{00}}{a^3}$$

$$0 = 4\mu a_{2m} + \frac{24\mu}{a^5}A_{2m} - \frac{B_{2m}}{a^3}\left[6\lambda + 4\mu\left(\alpha_{-3} - 3\right)\right] \tag{2.13}$$

$$0 = 2aa_{2m} - \frac{8}{a^4}A_{2m} + \left(\alpha_{-3} - 6\right)\frac{B_{2m}}{a^2}$$

The boundary $\tau_{r\varphi} = 0$ on $r = a$ leads to the same condition as the third of Eqs. (2.13) and may therefore be ignored. From Eq. (2.8), $\alpha_{-3} = (3\lambda + 8\mu)/\mu$

Equations (2.13) yield the amplitudes

$$A_{00} = -\frac{a^3 a_{00}}{2\mu}(3\lambda + 2\mu)$$

$$A_{2m} = \frac{6a^5 a_{2m}(\lambda + \mu)}{9\lambda + 14\mu} \tag{2.14}$$

$$B_{2m} = \frac{10a^3 a_{2m}\mu}{9\lambda + 14\mu}$$

Calculating the hoop stress σ_θ from the third of Eqs. (2.6) and introducing the amplitudes given in Eqs. (2.14),

$$\sigma_\theta = 3a_{00}(3\lambda + 2\mu) + \frac{30\mu(\lambda + 2\mu)}{9\lambda + 14\mu}\left(a_{20} + 6a_{22}\right) - \frac{120\mu(\lambda + \mu)}{9\lambda + 14\mu}\Sigma a_{2m}Y_{2m} \tag{2.15}$$

Also, since $\sigma_r + \sigma_\theta + \sigma_\varphi = (3\lambda + 2\mu)\nabla\cdot\vec{s}$ and $\sigma_r = 0$ at $r = a$,

$$\sigma_\varphi = 3a_{00}(3\lambda + 2\mu) - \frac{30\mu(\lambda + 2\mu)}{9\lambda + 14\mu}\left(a_{20} + 6a_{22}\right) - \frac{60\lambda\mu}{9\lambda + 14\mu}\Sigma a_{2m}Y_{2m} \tag{2.16}$$

Inserting the values of a_{00} and a_{22} from Eqs. (2.4) and introducing explicit forms for the spherical harmonics,

$$\sigma_\theta = -\frac{3}{2}p_\ell + \frac{15}{2}\left(\frac{\lambda+2\mu}{9\lambda+14\mu}\right)\left(p_\ell+\sigma_z+\sigma_x-\sigma_y\right) - 15\left(\frac{\lambda+\mu}{9\lambda+14\mu}\right)\left[\left(p_\ell+\sigma_z\right)\left(3\cos^2\theta-1\right) + \left(\sigma_x-\sigma_y\right)\sin^2\theta\cos 2\phi\right] \tag{2.17}$$

$$\sigma_\varphi = -\frac{3}{2}p_\ell - \frac{15}{2}\left(\frac{\lambda+2\mu}{9\lambda+14\mu}\right)\left(p_\ell+\sigma_z+\sigma_x-\sigma_y\right) - \frac{15}{2}\left(\frac{\lambda}{9\lambda+14\mu}\right)\left[\left(p_\ell+\sigma_z\right)\left(3\cos^2\theta-1\right) + \left(\sigma_x-\sigma_y\right)\sin^2\theta\cos 2\phi\right] \tag{2.18}$$

For the case of azimuthal symmetry,

$$\sigma_\theta = -\frac{3}{2}p_\ell + \frac{15\left(p_\ell+\sigma_z\right)}{9\lambda+14\mu}\left[\frac{3}{2}\lambda+2\mu-3(\lambda+\mu)\cos^2\theta\right] \tag{2.19}$$

$$\sigma_\varphi = -\frac{3}{2}p_\ell - \frac{15\left(p_\ell+\sigma_z\right)}{9\lambda+14\mu}\left[\mu+\frac{3}{2}\lambda\cos^2\theta\right] \tag{2.20}$$

Finally, at the poles of the cavity, $\theta = 0, \pi$ and $\cos^2\theta = 1$. In this instance

$$\sigma_\theta = \sigma_\varphi = -\frac{3}{2}p_\ell - \frac{15\left(p_\ell+\sigma_z\right)}{9\lambda+14\mu}\left(\frac{3}{2}\lambda+\mu\right) \tag{2.21}$$

2.3 Specific Stress Distributions

Until now the initial stress system has remained unspecified. Some specific examples will now be considered. First, for the case of a uniform gravitational field with vanishing lateral displacement (i.e., $\sigma_z = -\rho gh$, $\epsilon_x - \epsilon_y = 0$), one finds the following set of stresses

$$\begin{aligned}\sigma_z &= (\lambda+2\mu)\epsilon_z = -\rho gh \\ \sigma_x &= \sigma_y = \lambda\epsilon_z = \frac{\lambda}{\lambda+2\mu}\sigma_z = -\frac{\lambda\rho gh}{\lambda+2\mu}\end{aligned} \tag{2.22}$$

The pressure is given by

$$p_{\ell} = -\frac{1}{3}\left(\sigma_z + 2\sigma_x\right) = -\frac{3\lambda+2\mu}{3(\lambda+2\mu)}\,\sigma_z = \begin{cases} -\frac{5}{9}\sigma_z, & \lambda = \mu \\ -\frac{2}{3}\sigma_z, & \lambda = 2\mu \end{cases} \tag{2.23}$$

Hence, the magnitude of the pressure is somewhat less than σ_z. Equation (2.19) now becomes

$$\sigma_\theta = -\frac{3}{2}p_{\ell} + \frac{20\mu\sigma_z}{(9\lambda+14\mu)(\lambda+2\mu)}\left[\frac{3}{2}\lambda + 2\mu - 3(\lambda+\mu)\cos^2\theta\right] \tag{2.24}$$

For the two cases $\lambda = \mu$ and $\lambda = 2\mu$,

$$\begin{aligned} \frac{\sigma_\theta}{\rho g h} &= -1.85(1 - 0.94\cos^2\theta), \quad \lambda = \mu \\ \frac{\sigma_\theta}{\rho g h} &= -1.78(1 - 0.79\cos^2\theta), \quad \lambda = 2\mu \end{aligned} \tag{2.25}$$

At the top and bottom of the cavity, $\cos^2\theta = 1$ and one obtains

$$\frac{\sigma_\theta}{\rho g h} = \begin{cases} -0.11, & \lambda = \mu \\ -0.38, & \lambda = 2\mu \end{cases} \tag{2.26}$$

It is clear from this result that the hoop stress may be only a few tenths of the lithostatic pressure. Since the cavity will split at its weakest point, it is this lowest value of the hoop stress which is relevant.

As a second illustration, it is shown that it is possible to find a reasonable stress field for which the hoop stress vanishes. Equation (2.19) takes the following forms for $\lambda = \mu$ and $\lambda = 2\mu$.

$$\sigma_\theta = -\frac{3}{2}p_{\ell} + \frac{15}{23}\left(p_{\ell} + \sigma_z\right)\left[\frac{3}{2} - 4P_2(\cos\theta)\right], \quad \lambda = \mu \tag{2.27}$$

$$\sigma_\theta = -\frac{3}{2}p_{\ell} + \frac{15}{16}\left(p_{\ell} + \sigma_z\right)\left[1 - 3P_2\cos\theta)\right], \quad \lambda = 2\mu \tag{2.28}$$

where $p_{\ell} = -\frac{1}{3}\left(\sigma_z + 2\sigma_x\right)$ Setting $\theta = 0$ and requiring $\sigma_\theta = 0$ yields

$$\sigma_\theta = 0 \quad \text{for} \begin{cases} \sigma_x/\sigma_z = 0.28, & \lambda = \mu \\ \sigma_x/\sigma_z = 0.33, & \lambda = 2\mu \end{cases} \tag{2.29}$$

For smaller ratios, the poles would actually be in tension.

Since such ratios are not unreasonable, it is clear that extreme care would have to be exercised in determining the stress field in the region where the cavity were to be constructed.

To determine the importance of anisotropy in such considerations, Eqs. (2.17) and (2.18) may be evaluated at $\theta = 0$. The result is:

$$\sigma_\theta\left(0^\circ\right) = -\frac{3}{2}p_{\ell} - \frac{15}{2(9\lambda + 14\mu)}\left[(3\lambda + 2\mu)\left(p_{\ell} + \sigma_z\right) - (\lambda + 2\mu)\left(\sigma_x - \sigma_y\right)\right] \tag{2.30}$$

$$\sigma_\varphi\left(0^\circ\right) = -\frac{3}{2}p_{\ell} - \frac{15}{2(9\lambda + 14\mu)}\left[(3\lambda + 2\mu)\left(p_{\ell} + \sigma_z\right) + (\lambda + 2\mu)\left(\sigma_x - \sigma_y\right)\right] \tag{2.31}$$

From this result it follows that either σ_θ or σ_φ will be increased by any asymmetry about the Z axis.

CHAPTER 3

THE STRESS DISTRIBUTION AROUND A PROLATE SPHEROIDAL CAVITY

3.1 Introduction

The analysis contained in the preceding chapter has given some indication of the dependence of the hoop stress upon the stress field initially present in the medium from which the cavity is excised. It is also desirable to have some understanding of the dependence of the hoop stress upon the shape of the cavity itself. The simplest nonspherical shape which admits of analytical treatment is the spheroidal cavity. Even this case results in considerable analytic complexity, and, as a result, attention has been confined to the case of a uniform gravitational field with vanishing lateral displacement. The result for an isotropic pressure field is obtained as before by setting Poisson's ratio equal to 1/2. On the basis of well-known intuitive notions of the stability of such cavities (e.g., the need for supporting mining tunnels), the shape is assumed to be that of a prolate spheroid with the major axis directed vertically (see Fig. 3). On the whole, the results bear out the intuitive notion that stresses are increased at points where the curvature of the bounding surface is increased. Comparing the results for the spheroidal cavity with those for the spherical cavity, it is found that the spheroidal shape results in a slightly larger compressive stress at the top and bottom of the cavity and less compressive stress at the sides of the cavity.

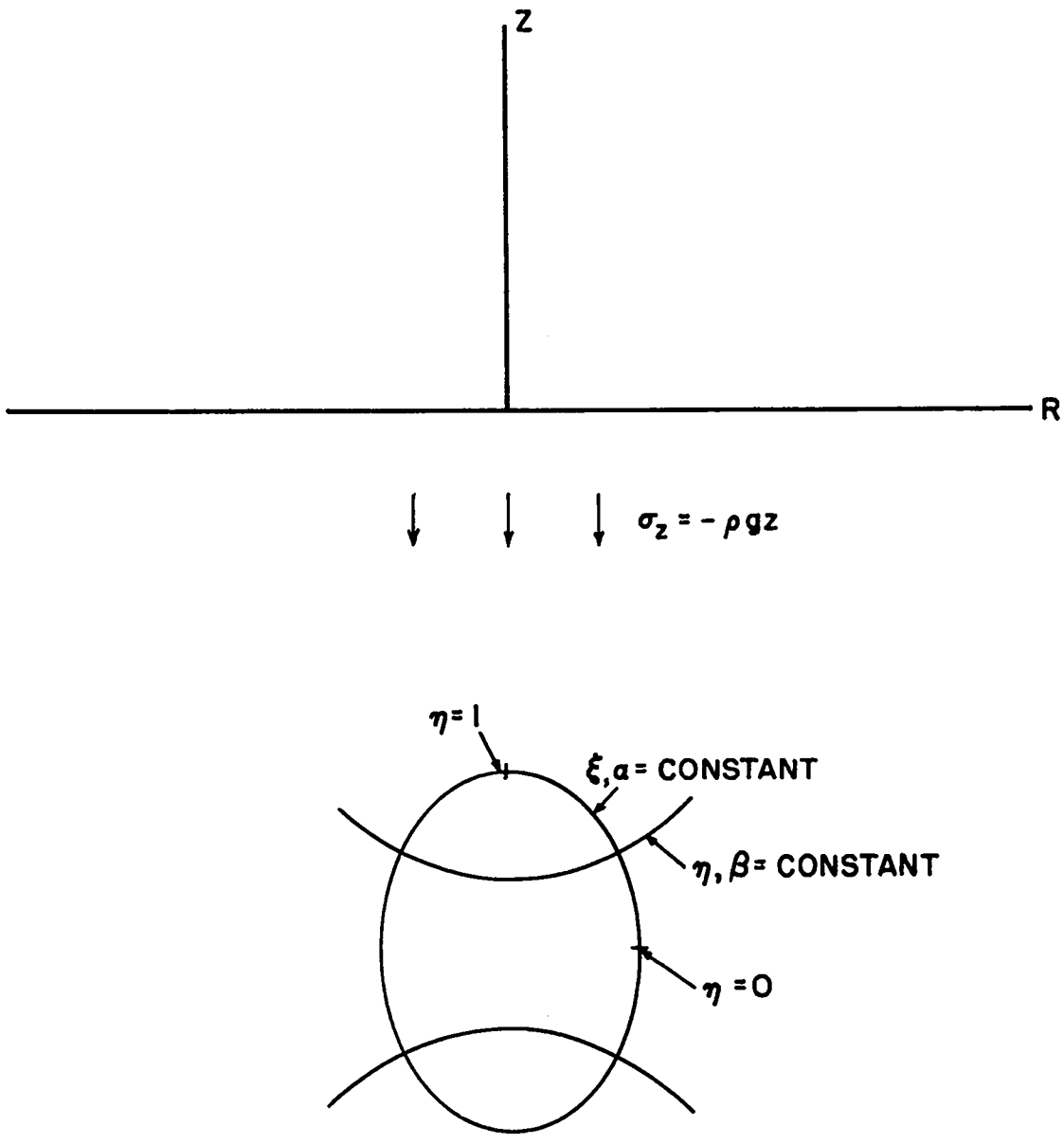

Fig. 3 Coordinate system for prolate spheroidal cavity.

3.2 Mathematical Formulation of the Problem

Since the vector equation for the static displacement of an elastic solid is not separable in prolate spheroidal coordinates, a somewhat more general technique than that employed in Chapter 2 is required.[5] The approach to be used here is to write a solution for the displacement in rectangular coordinates and then transform this expression to prolate spheroidal coordinates to calculate the stresses.

The transformation equations are

$$\begin{aligned} x &= \frac{a}{2}\sqrt{\left(\xi^2-1\right)\left(1-\eta^2\right)}\cos\gamma = \frac{a}{2}\sinh\alpha\,\sin\beta\,\cos\gamma \\ y &= \frac{a}{2}\sqrt{\left(\xi^2-1\right)\left(1-\eta^2\right)}\sin\gamma = \frac{a}{2}\sinh\alpha\,\sin\beta\,\sin\gamma \\ z &= \frac{a}{2}\xi\eta = \frac{a}{2}\cosh\alpha\,\cos\beta \end{aligned} \tag{3.1}$$

where a is the interfocal distance, and the prolate spheroidal surfaces are given by $\xi = \cosh\alpha = \text{constant}$. The equation to be solved is again Eq. (2.2) of the preceding chapter, which may also be written in the form

$$(\lambda+2\mu)\nabla(\nabla\cdot\vec{s}) - \mu\nabla\times\nabla\times\vec{s} = 0 \tag{3.2}$$

The solution is written in terms of the three scalar harmonic functions ϕ, θ and χ as

$$\vec{s} = \nabla\phi + \nabla\times\vec{k}\theta + z\nabla\chi - (3-4\sigma)\chi \tag{3.3}$$

where $\vec{k}$ is a unit vector along the vertical Z axis and σ is Poisson's ratio given by $\sigma = \lambda/2(\lambda+\mu)$. The purely shear solution θ may again be discarded. The procedure followed now is to decompose the displacement given by Eq. (3.3) into the prolate spheroidal coordinates (α, β, γ), calculate the stresses $\tau_{\alpha\alpha}$, $\tau_{\alpha\beta}$ and $\tau_{\beta\beta}$ and then express these results in the (ξ, η, γ) system. The slight computational advantage in this mixed approach is that two of the

metric coefficients are identical in the (α, β, γ) system while this is not the case in the (ξ, η, γ) system (see Appendix A).

As in Chapter 2 it is assumed that the initial stress field is derivable from the scalar potential

$$\phi^{(0)} = \frac{1}{2}\left(\epsilon_x x^2 + \epsilon_y y^2 + \epsilon_z z^2\right) \tag{3.4}$$

The form of this potential in terms of the eigenfunctions for prolate spheroidal coordinates is readily found to be

$$\phi^{(0)} = A\left[P_2(\xi) + P_2(\eta)\right] + B\left[P_2(\xi)P_2(\eta)\right] + C\left[P_2^2(\xi)P_2^2(\eta)\right]\cos 2\gamma + \text{const} \tag{3.5}$$

where

$$\begin{aligned} A &= \frac{a^2}{36}\nabla\cdot\vec{s} \\ B &= \frac{a^2}{72\mu}\left(2\sigma_z - \sigma_x - \sigma_y\right) \\ C &= \frac{a^2}{72\mu}\left(\sigma_x - \sigma_y\right) \end{aligned} \tag{3.6}$$

and the P_n^m are the usual Legendre functions of the first kind.

Decomposing the displacement in the (α, β, γ) system so that $\vec{s} = \vec{s}_\alpha + \vec{s}_\beta + \vec{s}_\gamma$, the strains are given by (see Appendix A)

$$\begin{aligned} \epsilon_{\alpha\alpha} &= \frac{2h}{a}\left(\bar{\xi}\frac{\partial s_\alpha}{\partial \xi} + h^2\eta\bar{\eta}s_\beta\right) \\ \epsilon_{\beta\beta} &= \frac{2h}{a}\left(-\bar{\eta}\frac{\partial s_\beta}{\partial \eta} + h^2\xi\bar{\xi}s_\alpha\right) \\ \epsilon_{\alpha\beta} &= \frac{1}{a}\left[\bar{\xi}\frac{\partial}{\partial \xi}\left(hs_\beta\right) - \bar{\eta}\frac{\partial}{\partial \eta}\left(hs_\alpha\right)\right] \end{aligned} \tag{3.7}$$

where $h^2 \equiv \left(\xi^2 - \eta^2\right)^{-1}$, $\bar{\xi}^2 \equiv \xi^2 - 1$, $\bar{\eta}^2 \equiv 1 - \eta^2$. Since the only case to be considered possesses azimuthal symmetry, the γ dependence may be ignored throughout.

The relevant tensor components of the generalized Hooke's law are given by[6]

$$\begin{aligned} \tau_{\alpha\alpha} &= \lambda \nabla \cdot \vec{s} + 2\mu \epsilon_{\alpha\alpha} \\ \tau_{\beta\beta} &= \lambda \nabla \cdot \vec{s} + 2\mu \epsilon_{\beta\beta} \\ \tau_{\alpha\beta} &= 2\mu \epsilon_{\alpha\beta} \end{aligned} \tag{3.8}$$

It is now necessary to find potentials ϕ and χ such that the stresses calculated from the displacement in Eq. (3.3) will exactly cancel at the surface of the cavity those stresses obtained from the potential $\phi^{(0)}$ of Eq. (3.4). From Eq. (3.3) it is seen that the displacements are of two types, those derivable from a scalar potential ϕ in the ordinary way and those derived from the scalar χ functions.

For the ϕ potential, the stresses are found from Eqs. (3.3), (3.7) and (3.8) to be

$$\begin{aligned} \tau_{\alpha\alpha} &= \frac{8\mu}{a^2}\left[\bar{\xi}^2 h^2 \phi_{\xi\xi} + \bar{\eta}^2 h^4 \left(\xi\phi_\xi - \eta\phi_\eta\right)\right] \\ \tau_{\beta\beta} &= \frac{8\mu}{a^2}\left[\bar{\eta}^2 h^2 \phi_{\eta\eta} + \bar{\xi}^2 h^4 \left(\xi\phi_\xi - \eta\phi_\eta\right)\right] \\ \tau_{\alpha\beta} &= \frac{8\mu}{a^2}\bar{\xi}\bar{\eta}\left[-h^2 \phi_{\xi\eta} + h^4 \left(\xi\phi_\eta - \eta\phi_\xi\right)\right] \end{aligned} \tag{3.9}$$

where the subscripts ξ and η refer to partial differentiation with respect to these variables.

A similar calculation for the χ function shows that the stresses are given by

$$\tau_{\alpha\alpha} = \frac{4\mu}{a}\left[2\sigma h^2\left(-\bar{\eta}^2\xi\chi_\eta + \bar{\xi}^2\eta\chi_\xi\right) + \xi\eta\bar{\eta}^2h^4\left(\xi\chi_\xi - \eta\chi_\eta\right) + \bar{\xi}^2\eta h^2\left(\xi\chi_{\xi\xi} - 2\chi_\xi\right)\right]$$

$$\tau_{\beta\beta} = \frac{4\mu}{a}\left[2\sigma h^2\left(-\bar{\xi}^2\eta\chi_\xi + \bar{\eta}^2\xi\chi_\eta\right) - \eta\xi\bar{\xi}^2h^4\left(\eta\chi_\eta - \xi\chi_\xi\right) + \bar{\eta}^2\xi h^2\left(\eta\chi_{\eta\eta} - 2\chi_\eta\right)\right] \qquad (3.10)$$

$$\tau_{\alpha\beta} = \frac{4\mu}{a}\bar{\xi}\bar{\eta}h^2\left[-\xi\eta\chi_{\xi\eta} + (1-2\sigma)\left(\xi\chi_\xi + \eta\chi_\eta\right) - h^2\xi\eta\left(\eta\chi_\xi - \xi\chi_\eta\right)\right]$$

The stresses on the surface of the cavity due to the initial stress distribution are found by substituting Eq. (3.4) into Eqs. (3.9). For the case in which C = 0 (aximuthal symmetry), and noting that $\nabla\cdot\vec{s}^{(0)} = \nabla^2\phi^{(0)} = 36\ A/a^2$ one finds

$$\tau^{(0)}_{\alpha\alpha} = \frac{12A}{a^2}(3\lambda + 2\mu) + \frac{12\mu B}{a^2}\left[3\bar{\xi}^2\xi^2h^2 - \left(3\xi^2 - 2\right)\right]$$

$$\tau^{(0)}_{\beta\beta} = \frac{12A}{a^2}(3\lambda + 2\mu) + \frac{12\mu B}{a^2}\left[-3\bar{\xi}^2\xi^2h^2 + \left(3\xi^2 - 1\right)\right] \qquad (3.11)$$

$$\tau^{(0)}_{\alpha\beta} = \frac{-36\mu B}{a^2}\bar{\xi}\xi\bar{\eta}\eta h^2$$

It is now necessary to find those functions ϕ and χ which have the same η dependence around the surface of the cavity and then to add together the appropriate linear combination of these solutions in order to cancel out the stresses $\tau^{(0)}_{\alpha\alpha}$ and $\tau^{(0)}_{\alpha\beta}$ at the cavity surface. Perhaps the easiest way to determine the proper functions is to calculate the stress $\tau_{\alpha\beta}$ from the third of Eqs. (3.9) and (3.10). According to the third of Eqs. (3.11), only those solutions having the dependence $\eta\bar{\eta}$ are admissible. The only solutions having such dependence are found to be

$$\phi_0 = P_0(\eta)Q_0(\xi)$$

$$\phi_2 = P_2(\eta)Q_2(\xi) \qquad (3.12)$$

$$\chi_1 = P_1(\eta)Q_1(\xi)$$

where the $Q_\eta(\xi)$ are the Legendre functions of the second kind.

The stresses resulting from these three functions are found from Eqs. (3.9) and (3.10) to be

ϕ_0 Solution

$$\tau_{\alpha\alpha} = \frac{4\mu}{a^2}\left(\frac{2\xi}{\bar{\xi}^2}h^2 + 2\xi h^4\right)$$

$$\tau_{\alpha\beta} = \frac{4\mu}{a^2}\eta\bar{\eta}\left(\frac{2}{\bar{\xi}}h^4\right) \tag{3.13}$$

$$\tau_{\beta\beta} = \frac{4\mu}{a^2}\left(-2\xi h^4\right)$$

ϕ_2 Solution

$$\tau_{\alpha\alpha} = \frac{4\mu}{a^2}\left\{3Q_0\left(2-3\xi^2\right) + \frac{3\xi\left(3\xi^2-4\right)}{\bar{\xi}^2} + h^2\left[9Q_0\xi^2\bar{\xi}^2 + \frac{\xi\left(3\xi^2-1\right)\left(1-3\bar{\xi}^2\right)}{\bar{\xi}^2}\right] + 2\xi h^4\right\}$$

$$\tau_{\alpha\beta} = \frac{4\mu}{a^2}\eta\bar{\eta}\left[h^2\left(-9\xi\bar{\xi}Q_0 + \frac{9\xi^2-6}{\bar{\xi}}\right) + \frac{2}{\bar{\xi}}h^4\right] \tag{3.14}$$

$$\tau_{\beta\beta} = \frac{4\mu}{a^2}\left\{3Q_0\left(3\xi^2-1\right) - 9\xi + h^2\left[-9Q_0\xi^2\bar{\xi}^2 + 3\xi\left(1+3\bar{\xi}^2\right)\right] - 2\xi h^4\right\}$$

χ_1 Solution

$$\tau_{\alpha\alpha} = \frac{4\mu}{a}\left\{-2\xi(1-2\sigma) - \frac{\xi}{\bar{\xi}^2} + 2Q_0\left[\xi^2(1-2\sigma) - (1-\sigma)\right]\right.$$
$$\left. + h^2\left[(1-2\sigma)\left(-2Q_0\xi^2\bar{\xi}^2 + 2\xi^3 - \xi^3\right) + \frac{\xi^3}{\bar{\xi}^2}\right] + \xi^3 h^4\right\}$$

$$\tau_{\alpha\beta} = \frac{4\mu}{a}\eta\bar{\eta}\left[\bar{\xi}(1-2\sigma)\left(2\xi Q_0 - 2 - \frac{1}{\bar{\xi}^2}\right)h^2 + \frac{\xi^2}{\bar{\xi}}h^4\right] \qquad (3.15)$$

$$\tau_{\beta\beta} = \frac{4\mu}{a}\left\{2\xi(2\sigma-1)\left(\xi Q_0 - 1\right) - 2\sigma Q_0 + h^2\left[2\xi^2\bar{\xi}^2 Q_0(1-2\sigma) + \xi(3-2\sigma)\right.\right.$$
$$\left.\left. + 2\xi^3(2\sigma-1)\right] - \xi^3 h^4\right\}$$

For a uniform field with no lateral displacement (the case considered in Chapter 2) the constants of Eqs. (3.6) are

$$A = \frac{B}{2} = -\frac{\rho g L a^2}{36(\lambda+2\mu)}, \quad C = 0 \qquad (3.16)$$

and the initial field is

$$\frac{\tau^{(0)}_{\alpha\alpha}}{\rho g L} = -\left(1 - \frac{1-2\sigma}{1-\sigma}\xi^2\right) - \frac{1-2\sigma}{1-\sigma}\xi^2\bar{\xi}^2 h^2$$

$$\frac{\tau^{(0)}_{\alpha\beta}}{\rho g L} = \frac{1-2\sigma}{1-\sigma}\bar{\xi}\xi\bar{\eta}\eta h^2 \qquad (3.17)$$

$$\frac{\tau^{(0)}_{\beta\beta}}{\rho g L} = -\left(\frac{\sigma}{1-\sigma} + \frac{1-2\sigma}{1-\sigma}\xi^2\right) - \frac{1-2\sigma}{1-\sigma}\xi^2\bar{\xi}^2 h^2$$

It is now necessary to form a linear superposition of the stresses $\tau_{\alpha\alpha}$ and $\tau_{\alpha\beta}$ given in Eqs. (3.13), (3.14), (3.15) and (3.17) in order to satisfy the boundary condition of vanishing normal and tangential stress on the surface

of the cavity. Rather than attempt to carry this through in general, a series of numerical calculations were performed[7] for various values of λ, μ and ξ. These results are shown in Fig. 4 and are discussed below.

3.3 Discussion of Numerical Results

Figure 4 shows in graphical form the results of the numerical determination of the hoop stress at the top ($\eta = 1$) and side ($\eta = 0$) of the cavity for various values of cavity eccentricity. More specifically, the ratio of hoop stress to lithostatic pressure, $\tau_{\beta\beta}/\rho gL$, is plotted vs s, the ratio of minor to major axis. The values for $s = 1$ agree with the results for the spherical cavity considered in the previous chapter. The results for $\sigma = 1/2$ correspond to the solution for an isotropic pressure field. The slight difference in the results for $\sigma = 1/3$ and $\sigma = 1/4$, the region of values applicable to earth, shows that the calculation is quite insensitive to variation of the elastic parameters. The results are in agreement with the intuitive notion of stress concentration being increased by increasing curvature. In the present case the ellipsoidal cavity shape tends to equalize the hoop stress around the cavity surface at the initial field value ρgL and thus makes less likely a splitting of the cavity walls when a pressure is introduced within the cavity.

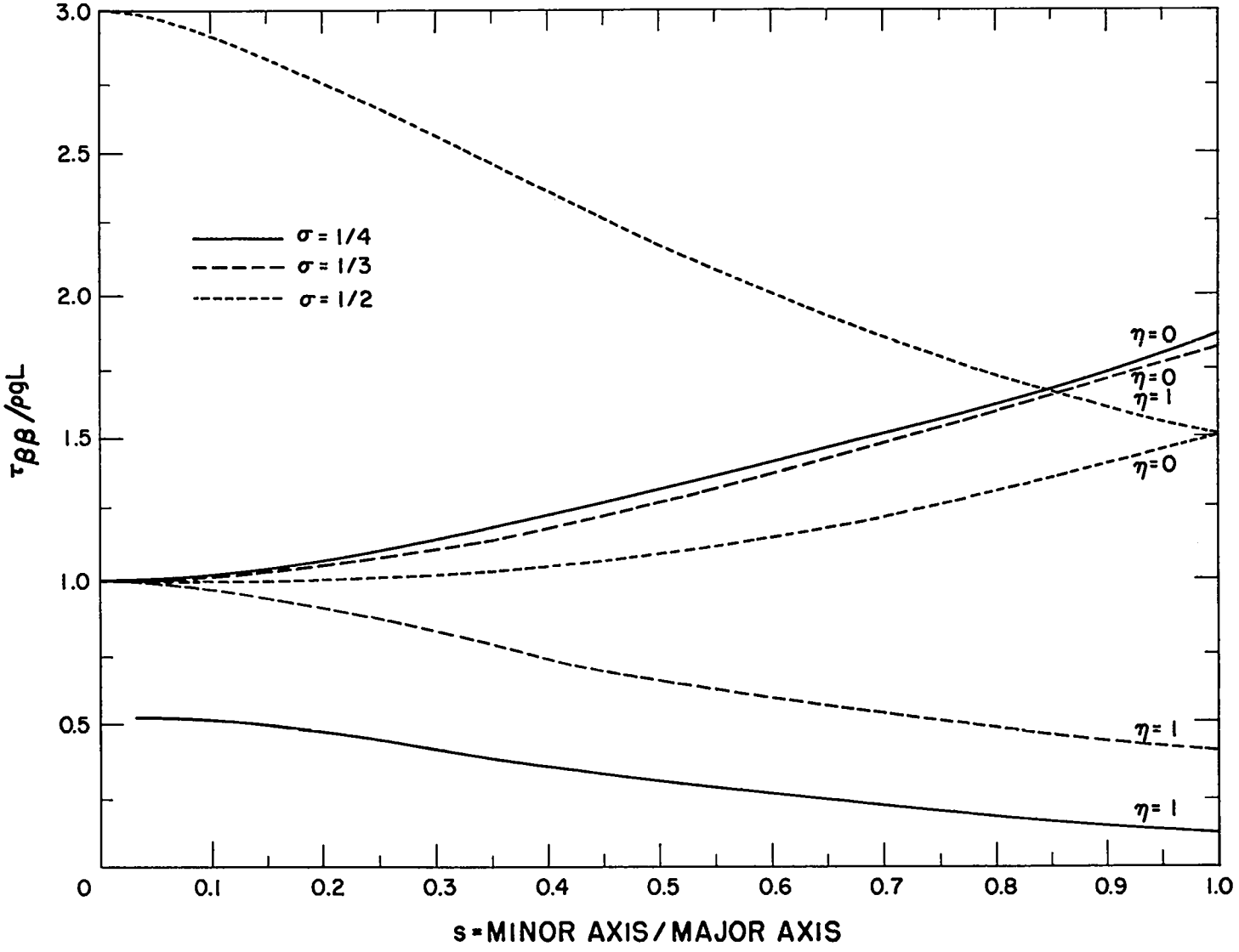

Fig. 4 Hoop stress vs eccentricity for prolate spheroidal cavity.

CHAPTER 4

THE PLASTIC EXPANSION OF A SPHERICAL CAVITY

4.1 Introduction

In cases where the cavity is not large enough to ensure elastic expansion, the problem is, of course, extremely complicated. For cavities not too much smaller than that required for purely elastic deformation, there appears a region of plastic flow bounded by a spherical surface beyond which the expansion is still elastic. For still smaller initial cavity radii, the temperature of the gas will be high enough to cause melting and vaporization of the cavity wall. An attempt to follow this process by a machine computation has been made by Nuckolls.[8] The discussion in the present chapter is far less ambitious and merely summarizes the calculation of the plastic expansion of a spherical cavity and applies the results to the problem in question. When numerical values for the parameters involved are substituted into the results, one finds a remarkable agreement with the published data on the expansion of the cavity formed in the Rainier event.[9] Determination of whether or not this is merely fortuitous must await the publication of similar data on other underground events.

4.2 Mathematical Formulation

When the pressure within the cavity is larger than that allowed for a

purely elastic expansion of the cavity wall, a zone of plastic expansion is formed. It has been found that this phenomenon can be discussed fairly well in terms of the theory of plasticity,[10] in which it is postulated that when the difference between any two of the principal stresses reaches a certain critical value (the yield stress of the material), the material no longer presents any resistance and flows like a perfect fluid. This flow persists out to a distance at which the difference in principal stresses has decreased to reach the yield stress. Beyond this distance the displacement is again elastic. Since the region of elastic expansion is the easiest to treat, it will be discussed first.

4.2a Elastic Region

Consider the case of a spherical shell of elastic material as shown in Fig. 5. In the final result the outer radius b will be allowed to tend to infinity while the external pressure p_1 remains constant. This will result in an isotropic stress distribution at large distances from the cavity. Assuming that the pressure p_0 within the cavity is small enough to ensure only elastic expansion, a solution to the equation for the static displacement of an elastic solid

$$(\lambda+\mu)\nabla(\nabla\cdot\vec{s}) - \mu\nabla^2\vec{s} = 0 \tag{4.1}$$

is again required. Decomposing the displacement $\vec{s}$ according to

$$\vec{s} = \vec{s}_1 + \vec{s}_2, \quad \vec{s}_1 = \nabla\varphi, \quad \vec{s}_2 = r^2\nabla\omega + \alpha r\omega, \quad \nabla^2\varphi = \nabla^2\omega = 0$$

as in Chapter 2, one finds that the appropriate displacement potentials are

$$\varphi = \varphi_{-1} = \frac{A}{r}, \quad \omega = \omega_0 = \text{const} = B'$$

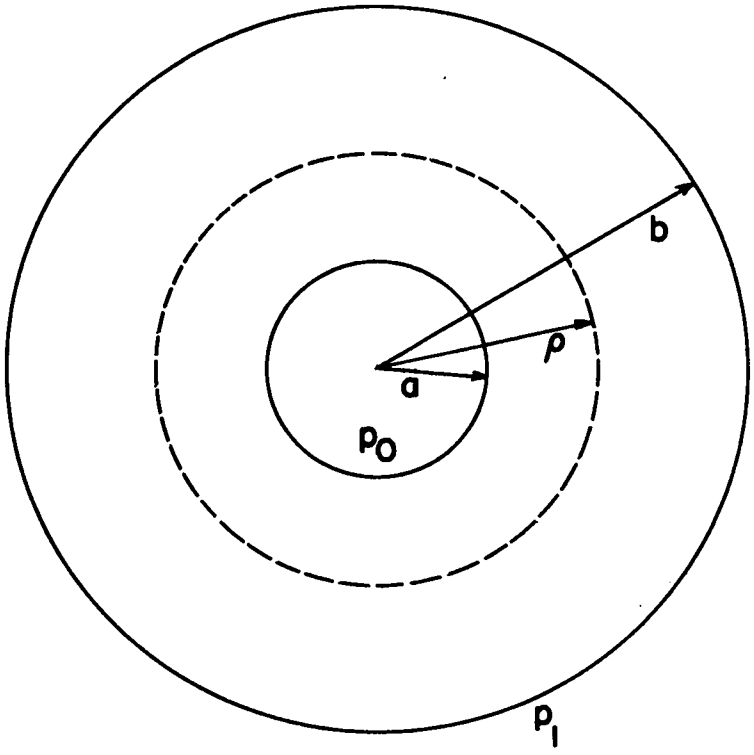

Fig. 5 Plastic region within a spherical elastic shell.

Hence,

$$\vec{s} = \vec{a}_r\left(-\frac{A}{r^2} + Br\right), \quad B \equiv \alpha B' \tag{4.2}$$

One also finds

$$\nabla\cdot\vec{s} = 3B$$

The stresses are given by

$$\sigma_r = \lambda\nabla\cdot\vec{s} + 2\mu\frac{\partial s_r}{\partial r} = (3\lambda + 2\mu)B + \frac{4\mu A}{r^3}$$

$$\sigma_\theta = \lambda\nabla\cdot\vec{s} + 2\mu\frac{s_r}{r} = (3\lambda + 2\mu)B - \frac{2\mu A}{r^3} \tag{4.3}$$

The boundary conditions are

$$\sigma_r = -p_0, \quad r = a$$

$$\sigma_r = -p_1, \quad r = b$$

In order to satisfy these boundary conditions it is found that the constants A and B must have the values

$$A = \frac{(p_0 - p_1)b^3}{4\mu\left(1 - b^3/a^3\right)}, \quad B = -\frac{\left(p_0 - p_1 b^3/a^3\right)}{(3\lambda + 2\mu)\left(1 - b^3/a^3\right)} \tag{4.4}$$

Noting that the Lamé constants λ and μ are related to the Young's modulus E and Poisson's ratio σ by

$$(3\lambda + 2\mu) = E/(1 - 2\sigma), \quad 2\mu = E/(1 + \sigma)$$

the radial displacement takes the form

$$s_r = -\frac{p_1(1-2\sigma)}{E}r + \frac{(p_0 - p_1)}{2E\left(b^3/a^3 - 1\right)}\left[(1+\sigma)\frac{b^3}{r^3} + 2(1-2\sigma)r\right] \tag{4.5}$$

Since the pressure p_1 is to be thought of as being turned on before the pressure p_0 is introduced into the cavity, the displacement of interest is the additional displacement proportional to p_0, or

$$s_r = \frac{p_0}{2E\left(b^3/a^3 - 1\right)}\left[(1+\sigma)\frac{b^3}{r^2} + 2(1-2\sigma)r\right] \tag{4.6}$$

The stresses become

$$\begin{aligned} \sigma_r &= -p_1 - \frac{p_0 - p_1}{b^3/a^3 - 1}\left(\frac{b^3}{r^3} - 1\right) \\ \sigma_\theta &= -p_1 + \frac{p_0 - p_1}{b^3/a^3 - 1}\left(\frac{b^3}{2r^3} + 1\right) \end{aligned} \tag{4.7}$$

In the limit $b \to \infty$ the displacement and stresses are

$$s_r = \frac{p_0}{2E}(1+\sigma)\frac{a^3}{r^2} \tag{4.8}$$

$$\begin{aligned} \sigma_r &= -p_1 - (p_0 - p_1)a^3/r^3 \\ \sigma_\theta &= -p_1 + (p_0 - p_1)a^3/2r^3 \end{aligned} \tag{4.9}$$

At the surface of the cavity ($r = a$) one finds

$$\begin{aligned} \sigma_r &= -p_0 \\ \sigma_\theta &= \frac{1}{2}(p_0 - 3p_1) \end{aligned} \tag{4.10}$$

and the well-known condition for the vanishing of the hoop stress

$$p_0 = 3p_1 \tag{4.11}$$

is obtained.

4.2b Plastic Region

Employing the yield condition $\sigma_\theta - \sigma_r = Y$, and noting from Eqs. (4.10) that in the elastic region

$$\sigma_\theta - \sigma_r = \frac{3}{2}\left(p_0 - p_1\right) \tag{4.12}$$

the internal pressure necessary to produce plastic yielding is

$$p_0 = p_1 + \frac{2}{3}Y \tag{4.13}$$

Comparing Eqs. (4.11) and (4.13), one finds that if $p_1 > \frac{1}{3}Y$, there will be plastic flow before fracture. For salt[11] and tuff,[12] both with a density ~ 2 gm/cm^3 and yield stress $\sim 10^8$ dynes/cm^2, one finds that there will be plastic yielding before fracture at burial depths greater than about 200 meters.

Turning now to a more detailed analysis of the plastic expansion of a spherical cavity, the yield condition

$$\sigma_\theta - \sigma_r = Y \tag{4.14}$$

where Y is the yield stress of the material is employed. At the elastic-plastic interface $r = \rho$ (see Fig. 5) one can employ the elastic expressions for σ_r, σ_θ and s_r, except that the constant internal pressure p_0 is replaced by some effective pressure p'. This effective pressure can be expressed in terms of Y by introducing Eqs. (4.9) into Eq. (4.14). There results

$$\left(\sigma_\theta - \sigma_r\right)\Big|_{r=\rho} = \frac{3}{2}\frac{a^3}{\rho^3}\left(p' - p_1\right) = Y \tag{4.15}$$

Hence,

$$p' = p_1 + \frac{2}{3}\frac{\rho^3}{a^3}Y \tag{4.16}$$

Inserting this result into Eqs. (4.9),

$$\sigma_r = -p_1 - \frac{2}{3}Y\frac{\rho^3}{r^3}$$

$$\sigma_\theta = -p_1 + \frac{1}{3}Y\frac{\rho^3}{r^3} \tag{4.17}$$

From Eq. (4.8), the displacement is seen to be,

$$s_r = \frac{1}{3}\frac{Y}{E}(1+\sigma)\frac{\rho^3}{r^2} \tag{4.18}$$

where again the initial displacement due to the pressure p_1 has been subtracted. For use at a later point, the derivative

$$\left.\frac{\partial s_r}{\partial \rho}\right|_{r=\rho} = \frac{Y}{E}(1+\sigma) \tag{4.19}$$

is also recorded.

In obtaining the displacements in the plastic region, the Prandtl-Reuss flow equations which relate the rate of change of the strain tensor to the rate of change of the stress tensor are assumed to hold. The Prandtl-Reuss equations are

$$\dot{\epsilon}_r = \frac{1}{E}\left[(1+\sigma)\dot{\sigma}_r - 3\sigma\bar{\sigma}\right] + \lambda\left(\sigma_r - \sigma\right)$$

$$\dot{\epsilon}_\theta = \frac{1}{E}\left[(1+\sigma)\dot{\sigma}_\theta - 3\sigma\bar{\sigma}\right] + \lambda\left(\sigma_\theta - \sigma\right) \qquad (4.20)$$

$$\dot{\epsilon}_\varphi = \frac{1}{E}\left[(1+\sigma)\dot{\sigma}_\varphi - 3\sigma\bar{\sigma}\right] + \lambda\left(\sigma_\varphi - \sigma\right)$$

where $\epsilon_r = \partial s_r/\partial r$, $\epsilon_\theta = s_r/r$, $\bar{\sigma} = \frac{1}{3}\left(\sigma_r + 2\sigma_\theta\right)$, $\epsilon_\varphi = \epsilon_\theta$, $\sigma_\varphi = \sigma_\theta$.

Adding Eqs. (4.20)

$$\dot{\epsilon}_r + 2\dot{\epsilon}_\theta = \frac{3}{E}(1-2\sigma)\dot{\bar{\sigma}} \qquad (4.21)$$

It has been found convenient to regard the total time derivatives, $\dot{\epsilon}_r$, etc., as derivatives with respect to a function which increases monotonically with time, particularly with respect to the radius of the elastic-plastic interface $r = \rho$. Hence, considering all stresses and strains to be functions of r and ρ,

$$\dot{\epsilon}_r(r,\rho) = \frac{d\epsilon_r}{d\rho} = \frac{\partial\epsilon_r}{\partial\rho} + \frac{\partial\epsilon_r}{\partial r}\frac{dr}{d\rho} = \frac{\partial\epsilon_r}{\partial\rho} + \dot{s}_r\frac{\partial\epsilon_r}{\partial r} \qquad (4.22)$$

Also,

$$\dot{s}_r = \frac{ds_r}{d\rho} = \frac{\partial s_r}{\partial\rho} + \dot{s}_r\frac{\partial s_r}{\partial r} \qquad (4.23)$$

so that

$$\dot{s}_r = \frac{\partial s_r/\partial\rho}{1 - \partial s_r/\partial r} \qquad (4.24)$$

Now, from the definition of $\bar{\sigma}$,

$$\dot{\bar{\sigma}} = \frac{1}{3}\left(\dot{\sigma}_r + 2\dot{\sigma}_\theta\right) = \frac{1}{3}\left[\left(\frac{\partial\sigma_r}{\partial\rho} + \dot{s}_r\frac{\partial\sigma_r}{\partial r}\right) + 2\left(\frac{\partial\sigma_\theta}{\partial\rho} + \dot{s}_r\frac{\partial\sigma_\theta}{\partial r}\right)\right] \qquad (4.25)$$

The stresses in the plastic region are obtained from the equilibrium equation

$$\frac{\partial \sigma_r}{\partial r} + 2\frac{(\sigma_r - \sigma_\theta)}{r} = 0 \tag{4.26}$$

Setting $\sigma_\theta - \sigma_r = Y$ and integrating,

$$\sigma_r = 2Y \ln r + \text{const} \tag{4.27}$$

Since the stresses at $r = \rho$ are just small enough for the elastic equations (4.15) to be applicable, the constant of integration is readily evaluated, and the radial stress at all points within the plastic region is given by

$$\sigma_r = -p_1 + 2Y \ln\left(\frac{r}{\rho}\right) - \frac{2}{3}Y \tag{4.28}$$

From this expression one obtains the important result that the internal pressure p_0 required to produce a plastic zone to a radius ρ is

$$p_0 = p_1 - 2Y \ln\left(\frac{a}{\rho}\right) + \frac{2}{3}Y \tag{4.29}$$

Also, from the yield condition,

$$\sigma_\theta = Y - p_1 + 2Y \ln\left(\frac{r}{\rho}\right) - \frac{2}{3}Y$$

The derivatives of σ_r and σ_θ with respect to ρ may now calculated and one finds from Eq. (4.29),

$$\dot{\bar{\sigma}} = 2Y\left(-\frac{1}{\rho} + \frac{\dot{s}_r}{r}\right) \tag{4.30}$$

From Eq. (4.21)

$$\frac{\partial \dot{s}_r}{\partial r} + 2\frac{\dot{s}_r}{r} = \frac{6Y(1-2\sigma)}{E}\left(-\frac{1}{\rho} + \frac{\dot{s}_r}{r}\right) \tag{4.31}$$

This first-order linear differential equation is readily solved to first order in Y/E. Since this ratio is of the order of 10^{-2} for both salt and tuff, it seems quite reasonable to assume that higher order terms may be neglected.

At the elastic-plastic interface $\dot{s}_r$ is given by Eq. (4.19). This allows determination of the integration constant arising in the solution of Eq. (4.31). The solution to first order in Y/E is

$$\dot{s}_r = \frac{ds_r}{d\rho} = \frac{Y}{E}\left[3(1-\sigma)\frac{\rho^2}{r^2} - 2(1-2\sigma)\frac{r}{\rho}\right] \tag{4.32}$$

The motion of the inner surface of the cavity may be followed by setting $s_r = a - a_0$, where a_0 is the initial cavity radius and a the radius at any later time. Since one may only obtain a solution to the first order in Y/E, the right-hand side of Eq. (4.32) may be rewritten with $r = a_0$ so that the differential equation to be solved is

$$\frac{da}{d\rho} = \frac{Y}{E}\left[3(1-\sigma)\frac{\rho^2}{a_0^2} - 2(1-2\sigma)\frac{a_0}{\rho}\right] \tag{4.33}$$

This differential equation for a is solved subject to the "initial" condition that when the plastic zone is about to form, the displacement of the inner cavity wall is still given by Eq. (4.18) for elastic deformation, hence,

$$\rho = a_0, \quad a = a_0 + \frac{1}{3}\frac{Y}{E}(1+\sigma)a_0 \tag{4.34}$$

Equation (4.33) may be integrated immediately. Using the condition given by Eq. (4.34) one obtains

$$\frac{a}{a_0} = 1 + (1-\sigma)\frac{Y}{E}\frac{\rho^3}{a_0^3} - 2\frac{Y}{E}(1-2\sigma)\left[\ln\left(\frac{\rho}{a_0}\right) + \frac{1}{3}\right] \tag{4.35}$$

Considering the limit of small initial cavity radius $(a_0 \to 0)$

$$\frac{a}{\rho} = \sqrt[3]{\frac{3(1-\sigma)Y}{E}} \tag{4.36}$$

This relation, along with Eq. (4.29), which may be written

$$\frac{\rho}{a} = e^{(p_0 - p_1/2Y) - 1/3} \tag{4.37}$$

are the results of interest.

4.3 Numerical Example

It could hardly be expected that the highly idealized calculation outlined previously could be of use in a detailed study of the plastic expansion of a cavity. Furthermore, the exponential dependence of Eq. (4.37) leads one to expect that this result is not insensitive to a more refined treatment of the problem. The purpose of this section is merely to show that, with the help of recently published values for the parameters characterizing tuff,[12] an agreement does in fact exist between the energy released in the Rainier event and the resulting plastic deformation.

Solving Eq. (4.37) for the internal pressure:

$$p_0 = p_1 + 2Y\left(\ln\frac{\rho}{a} + \frac{1}{3}\right) \tag{4.38}$$

From Ref. 9, for the Rainier event, $\rho/a = 130/55 = 2.3$, and since the burial depth was 790 ft, $p_1 = 47$ bars. From Appendix B the yield stress is seen to depend upon overburden. Assuming a linear relationship, $Y = 265$ bars for an overburden of 47 bars. Inserting these results in Eq. (4.38),

$$p_0 = 715 \text{ bars.}$$

Assuming that the energy is spread uniformly throughout a cavity of

55 ft radius, and employing a γ of 1.3,

$$E = \frac{\left(4\pi a^3/3\right)p_0}{\gamma - 1} = 1.1 \text{ kt} \tag{4.39}$$

The radiochemistry yield for Rainier has been given as 1.7 kt. The 35 per cent of the energy unaccounted for in this result is quite close to the estimated amount (32 per cent) of energy involved in vaporization and melting of tuff.[12]

The parameters involved are not accurately enough known to justify a great deal of faith in the above results. Whether or not they can be used as the basis of a phenomenological approach to the problem must await the publication of data on other underground events.

It is also interesting to note that Eq. (4.36) predicts a ratio of final cavity radius to radius of plastic zone of 0.25, whereas the experimentally observed ratio is 0.44.

CHAPTER 5

RAYLEIGH WAVES GENERATED BY AN AIR BURST OVER A HOMOGENEOUS ELASTIC HALF-SPACE

5.1 Introduction

The present chapter is an attempt to resolve in a semiquantitative fashion an apparent paradox in the Latter hole concept, namely, its prediction of seismic wave amplitudes which are even less than those observed from past air bursts. When it is recognized that the shock wave from a typical air burst has a velocity parallel to the earth which is comparable to the velocity of seismic surface waves, it is clear that considerable energy may be fed into the earth as a result of resonance effects. It is the purpose of this chapter to investigate this possibility in terms of a somewhat simplified model.

As in the study of the surface waves generated by an explosion in an underground cavity, the idealization of a homogeneous elastic half-space has been made the basis of the calculation. After employing data from past test operations to construct a suitable analytic expression for the pressure distribution on the surface of the half-space, the result is readily obtained as a particular case of the general formulation developed in Chapter 1 for solving the problem of an explosion in a cavity.

It is found that the present calculation does predict a surface wave

which is larger in amplitude than that obtained from an explosion of the same energy in an underground cavity. The actual magnitude of the difference depends upon the value of the attenuation factor used to eliminate high frequencies. The resonance effect is clearly exhibited in the results of the analysis.

5.2 Mathematical Formulation

It has been found that a fairly reasonable fit to experimental data[13] (see Fig. 6) may be obtained by using the expression

$$p(r,t) = I_0 \frac{1}{\left[1+\frac{1}{8}(r/h)^2\right]^2} \delta\left(\frac{r}{c}-t\right) \tag{5.1}$$

where

$p(r,t)$ = pressure

I_0 = impulse at ground zero

h = height of burst

c = shock velocity

The shock velocity has been assumed constant (see Fig. 7). This undoubtedly represents the severest idealization in the calculation but was motivated by the same requirements which led to the choice of Eq. (5.1), namely, tractability of the integrations required in later phases of the calculation.

The frequency spectrum of the disturbance given by Eq. (5.1) is

$$\hat{p}(r,\omega) \equiv \int_{-\infty}^{\infty} dt e^{i\omega t} p(r,t) = \frac{I_0 e^{i\omega r/c}}{\left[1+\frac{1}{8}(r/h)^2\right]^2} \tag{5.2}$$

Introducing similar spectrum functions for the displacement and stresses

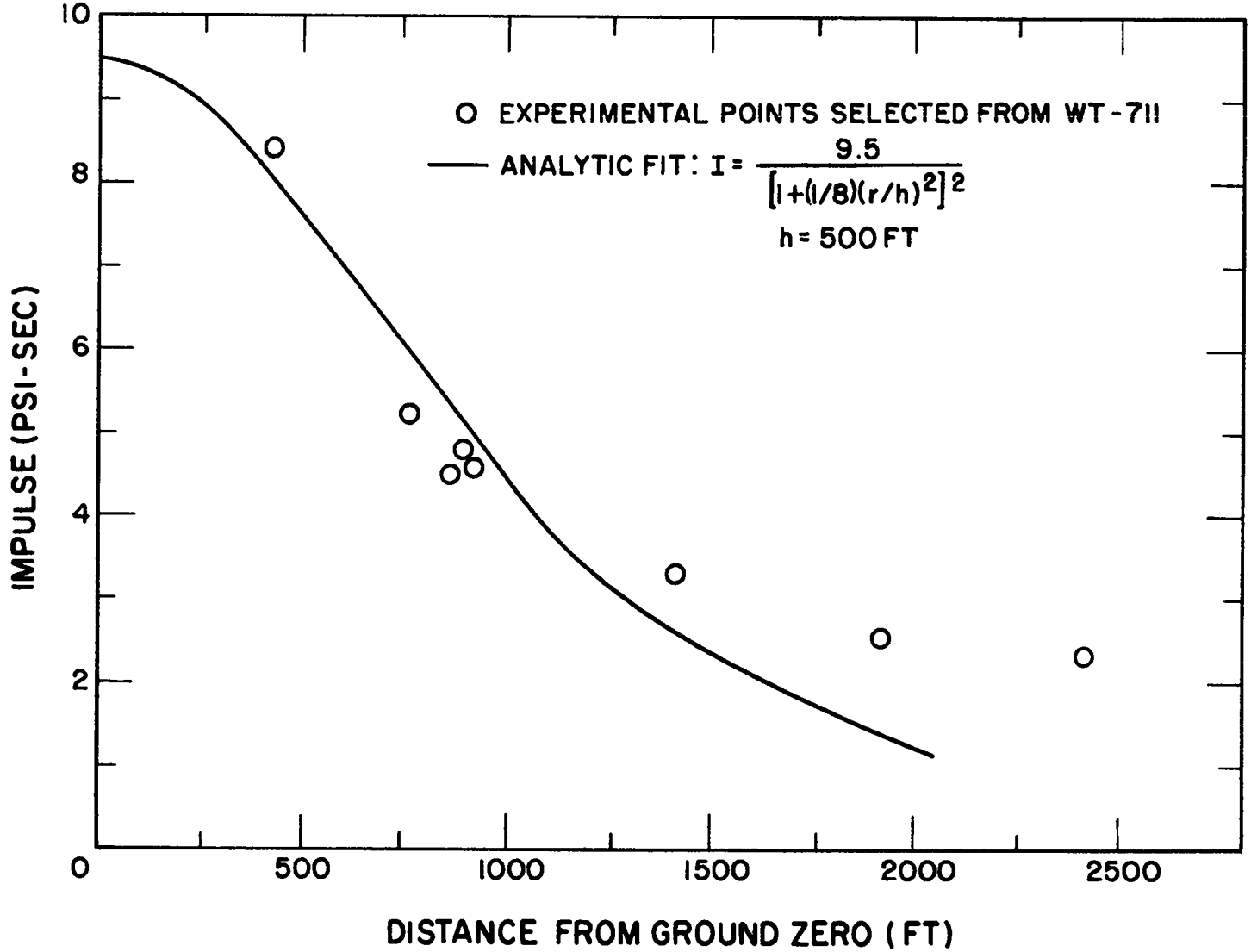

Fig. 6 Analytic fit to typical impulse-distance data.

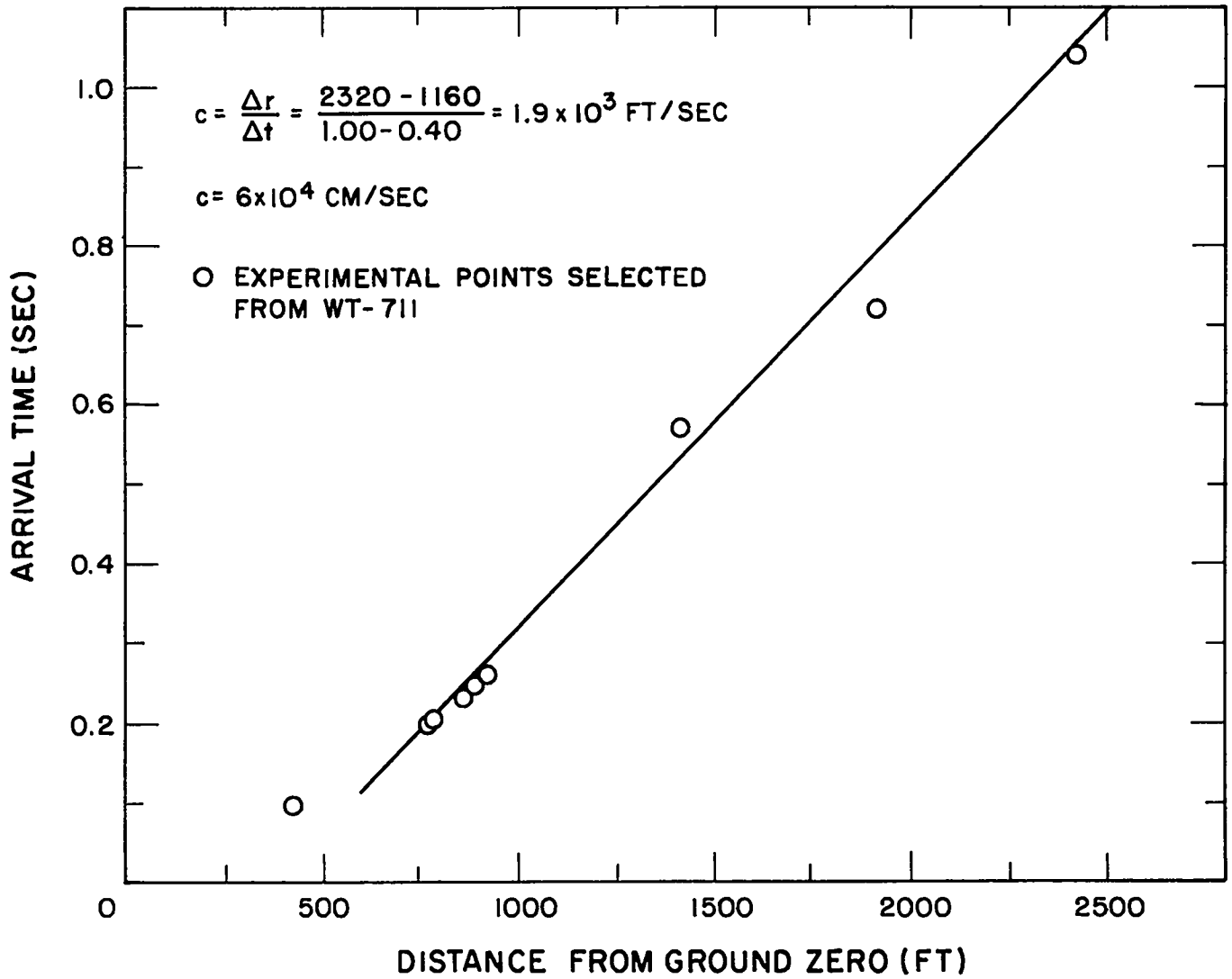

Fig. 7 Typical arrival time vs distance data.

of Chapter 1, these functions must satisfy boundary conditions similar to Eqs. (1.6), which are:

$$\hat{\tau}_{zr}(r, \omega) = \mu \left[\frac{\partial \hat{s}_r(r, z, \omega)}{\partial z} + \frac{\partial \hat{s}_z(r, z, \omega)}{\partial r} \right]_{z=0} = 0$$
$$\hat{\tau}_{zz}(r, \omega) = \lambda \nabla \cdot \hat{\vec{s}} + 2\mu \left. \frac{\partial \hat{s}_z(r, z, \omega)}{\partial z} \right|_{z=0} = -\hat{p}(r, \omega) \tag{5.3}$$

The displacements can again be written in terms of two scalar potentials having frequency spectra $\hat{\varphi}(r, z, \omega)$ and $\hat{\psi}(r, z, \omega)$ and Fourier-Bessel transforms given by

$$\hat{\varphi}(r, z, \omega) = \int_0^\infty \kappa d\kappa J_0(\kappa r) \Phi(\kappa, \omega) e^{i\zeta_L z}$$
$$\hat{\psi}(r, z, \omega) = \int_0^\infty \kappa d\kappa J_0(\kappa r) \Psi(\kappa, \omega) e^{i\zeta_T z} \tag{5.4}$$

A pair of simultaneous algebraic equations for $\Phi(\kappa, \omega)$ and $\Psi(\kappa, \omega)$ may now be obtained by substituting Eqs. (5.4) into Eqs. (5.3). One finds,

$$\left(-ik_T^2 \zeta_T + i\zeta_T^3\right)\Psi - \left(\frac{\lambda}{2\mu} k_L^2 + \zeta_L^2\right)\Phi = -\frac{1}{2\mu} \bar{p}(\kappa, \omega)$$
$$\left(-k_T^2 - 2\zeta_T^2\right)\Psi - 2i\zeta_L \Phi = 0 \tag{5.5}$$

where

$$\bar{p}(\kappa, \omega) = \int_0^\infty r dr J_0(\kappa r) \hat{p}(r, \omega) \tag{5.6}$$

The specific form of $\bar{p}(\kappa, \omega)$ will be considered subsequently.

Solving Eqs. (5.5) for Φ and Ψ and letting $\lambda = \mu$,

$$\Phi(\kappa, \omega) = \bar{p}(\kappa, \omega) \frac{\left(k_T^2 - 2\kappa^2\right)}{\mu F(\kappa)}$$

$$\Psi(\kappa, \omega) = -\bar{p}(\kappa, \omega) \frac{2i\zeta_L}{\mu F(\kappa)} \tag{5.7}$$

with $F(\kappa)$ again given by

$$F(\kappa) = \left(k_T^2 - 2\kappa^2\right)^2 + 4\zeta_L \zeta_T \kappa^2 \tag{5.8}$$

Introducing these results into Eqs. (5.4) and then calculating the vertical displacement from the relation

$$\hat{s}_z(r, 0, \omega) = \left.\frac{\partial \hat{\varphi}}{\partial z}\right|_{z=0} + k_T^2 \hat{\psi}(r, 0, \omega) + \left.\frac{\partial^2 \hat{\psi}}{\partial z^2}\right|_{z=0} \tag{5.9}$$

one finds,

$$\hat{s}_z(r, 0, \omega) = \frac{ik_T^2}{\mu} \int_0^\infty \kappa d\kappa J_0(\kappa r) \frac{\zeta_L \bar{p}(\kappa, \omega)}{F(\kappa)} \tag{5.10}$$

As in Chapter 1, the Rayleigh wave contribution to the displacement may be obtained by evaluating this integral in the complex plane and considering only the contribution from the residue at the zero of $F(\kappa)$. This calculation gives

$$\hat{s}_z(r, 0, \omega) = -\frac{2\pi}{\mu} \frac{k_T^2 k_R \sqrt{k_L^2 - k_R^2}}{F'\left(k_R\right)} H_0^{(1)}\left(k_R r\right) \bar{p}\left(k_R \omega\right) \tag{5.11}$$

Introducing $F'\left(k_R\right) = -4.64 k_T^2 k_R$ and $k_L^2 = 0.282 k_R^2$, one obtains

$$\hat{s}_z(r, 0, \omega) = \frac{1.14ik_R}{\mu} H_0^{(1)}\left(k_R r\right)\bar{p}\left(k_R, \omega\right) \tag{5.12}$$

Employing the asymptotic form of the Hankel function, the displacement in the far field is given in the form

$$s_z(r, 0, \tau) = \frac{0.29i}{\mu\sqrt{rc_R}} \int_0^\infty d\omega e^{-i(\omega\tau - \pi/4)} \sqrt{\omega}\, \bar{p}\left(k_R, \omega\right), \quad \tau = t - r/c \tag{5.13}$$

At this point it is convenient to rewrite Eq. (5.2) in the form

$$\hat{p}(r, \omega) = \frac{Ae^{i\omega r/c}}{\left(a^2 + r^2\right)^2} \tag{5.14}$$

where

$$A = 64h^4 I_0$$

$$a^2 = 8h^2$$

The calculation of the Fourier-Bessel transform is carried out in Appendix C, where it is shown that

$$\bar{p}\left(k_R, \omega\right) = i\frac{\pi}{4} A \frac{\omega}{ac} e^{-\omega a/c}\left[I_0\left(k_R a\right) - \frac{k_R c}{\omega} I_1\left(k_R a\right)\right] \tag{5.15}$$

where $I_n\left(k_R a\right)$ is the Bessel function of imaginary argument.
Substituting this result into Eq. (5.13) and again introducing the phenomenological attenuation factor $e^{-\alpha\omega}$ to eliminate the high frequencies,

$$s_z(r, 0, \tau) = -\frac{0.23A}{\mu ac\sqrt{rc_R}} \int_0^\infty d\omega e^{-i(\omega\tau - \pi/4)} e^{-(a/c + \alpha)\omega} \omega^{3/2}\left[I_0\left(\omega\frac{a}{c_R}\right) - \frac{c}{c_R} I_1\left(\omega\frac{a}{c_R}\right)\right] \tag{5.16}$$

It should be noted that without the term $e^{-\alpha\omega}$, this integral does not converge when $c = c_R$. These integrations could be carried out in terms of generalized hypergeometric functions of two variables and a graph of wave shape similar to that in Fig. 2. Since the domain of convergence of such expansions is not adequate to cover the range of τ values of interest and since a consideration of analytic continuation of these solutions is most likely unwarranted due to the approximate nature of the entire analysis, an evaluation of Eq. (5.16) at the single point $\tau = 0$ was decided upon. On the basis of the results of Chapter 1, one can infer that such a result will give the correct order of magnitude for the displacement. In this special case the integrations result in well known functions[14] and one obtains

$$s_z(r, 0, \tau)\Big|_{\tau=0} = \frac{-0.23e^{i\pi/4}A}{\mu ac\sqrt{rc_R}}\left(\frac{c_R}{a}\right)^{5/2}\sqrt{\frac{2}{\pi}}\frac{1}{p^2-1}\left[Q^2_{-1/2}(p) - \frac{c}{c_R}Q^2_{1/2}(p)\right] \tag{5.17}$$

where $p \equiv \frac{c_R}{c}(1+\alpha c/a)$ and the functions Q^{μ}_{ν} are the associated Legendre functions of the second kind.

5.3 Numerical Example

From Fig. 7 it is seen that a shock velocity $c = 0.6$ km/sec has been chosen from the experimental data. Since the burst height for the event from which the data has been taken was approximately 500 ft, giving $a = 4.3 \times 10^4$ cm, one finds $p = 17.1$. In obtaining this result, the values $c_R = 3.2$ km/sec and $\alpha = 1.59$ sec have again been used. Since the argument of the associated Legendre functions is so large, one may employ the asymptotic formula[15]

$$Q^{\mu}_{\nu}(z) \simeq \frac{e^{\mu\pi i}\sqrt{\pi}}{2^{\nu+1}}\frac{\Gamma(\nu+\mu+1)}{\Gamma(\nu+3/2)}z^{-\nu-1} \tag{5.18}$$

as a result one finds

$$Q^2_{-1/2}\ (17.1) = 0.41$$

$$Q^2_{1/2}\ (17.1) = 0.031$$

Taking the value of the impulse at ground zero to be $I_0 = 9.5$ psi-sec one finally obtains

$$s_z(r, 0, t)\Big|_{\tau=0} = \frac{70}{\sqrt{r}} \tag{5.19}$$

where r is in km and s_z in microns. This result predicts a displacement of 2.2 microns at 1000 km. According to Eq. (1.26) the maximum amplitude for a similar explosion (15 kt) in a cavity is 0.5 micron.

As in Chapter 1, the results of the present calculation depend upon the value chosen for the attenuation coefficient α. For the shock and Rayleigh wave velocities used, this dependence is about the same in both cases. More specifically, setting $\alpha = 0$ in the results of Chapter 1 increases the amplitude by a factor of about 20, and setting $\alpha = 0$ in the result of the present chapter increases the amplitude by a factor of about 15.

APPENDIX A

STRESS-STRAIN RELATIONS IN PROLATE SPHEROIDAL COORDINATES

The development of the equations of elasticity in prolate spheroidal coordinates is outlined in this appendix. A fuller discussion of the formulas for an arbitrary system of orthogonal coordinates may be found in Ref. 6.

For the sake of brevity, the rectangular and prolate spheroidal coordinates are redefined as $x = x_1$, $y = x_2$, $z = x_3$; $\alpha = u_1$, $\beta = u_2$, $\gamma = u_3$; $\xi = v_1$, $\eta = v_2$, $\gamma = v_3$. Then, Eqs. (3.1) are of the form

$$x_i = x_i(u_1, u_2, u_3) = x_i(v_1, v_2, v_3), \quad i = 1, 2, 3$$

and one may obtain the metric coefficients g_{ij} from the definition

$$g_{ij} = \sum_{k=1}^{3} \frac{\partial x_k}{\partial u_i} \frac{\partial x_k}{\partial u_j} \tag{A-1}$$

For the (α, β, γ) system, the nonvanishing coefficients are

$$\begin{aligned} g_{11} &= g_{\alpha\alpha} = \frac{a^2}{4}\left(\cosh^2\alpha - \cos^2\beta\right) = \frac{a^2}{4}\left(\xi^2 - \eta^2\right) \\ g_{22} &= g_{\beta\beta} = \frac{a^2}{4}\left(\cosh^2\alpha - \cos^2\beta\right) = \frac{a^2}{4}\left(\xi^2 - \eta^2\right) \\ g_{33} &= g_{\gamma\gamma} = \frac{a^2}{4}\sinh^2\alpha \sin^2\beta = \frac{a^2}{4}\bar{\xi}^2\bar{\eta}^2 \end{aligned} \tag{A-2}$$

For the (ξ, η, γ) system, the nonvanishing coefficients are

$$g_{11} = g_{\xi\xi} = \frac{a^2}{4} \frac{\xi^2 - \eta^2}{\xi^2 - 1}$$

$$g_{22} = g_{\eta\eta} = \frac{a^2}{4} \frac{\xi^2 - \eta^2}{1 - \eta^2} \tag{A-3}$$

$$g_{33} = g_{\gamma\gamma} = \frac{a^2}{4} \bar{\xi}^2 \bar{\eta}^2$$

The strains are given by

$$\epsilon_{ii} = \frac{\partial}{\partial u_i}\left(\frac{s_j}{\sqrt{g_{ii}}}\right) + \frac{1}{2g_{ii}} \sum_{\kappa=1}^{3} \frac{\partial g_{ii}}{\partial u_\kappa} \frac{s_\kappa}{\sqrt{g_{\kappa\kappa}}}$$

$$\epsilon_{ij} = \frac{1}{2\sqrt{g_{ii}g_{jj}}} \left[g_{ii} \frac{\partial}{\partial u_j}\left(\frac{s_i}{\sqrt{g_{ii}}}\right) + g_{jj} \frac{\partial}{\partial u_i}\left(\frac{s_j}{\sqrt{g_{jj}}}\right) \right] \tag{A-4}$$

The generalized Hooke's law is given by

$$\tau_{ij} = \lambda \nabla \cdot \vec{s} \delta_{ij} + 2\mu \epsilon_{ij} \tag{A-5}$$

with

$$\nabla \cdot \vec{s} = \frac{1}{\sqrt{g}} \sum \frac{\partial}{\partial \mu_\kappa}\left(\sqrt{g_{ii}g_{jj}}\, s_\kappa\right), \quad g \equiv g_{11}g_{22}g_{33}$$

Inserting the expressions for the metric coefficients given in Eqs. (A-2) and noting that

$$\frac{\partial}{\partial \alpha} = \bar{\xi} \frac{\partial}{\partial \xi}, \quad \frac{\partial}{\partial \beta} = -\bar{\eta} \frac{\partial}{\partial \eta} \tag{A-6}$$

the stresses become

$$
\begin{aligned}
\tau_{\alpha\alpha} &= \lambda\nabla\cdot\tilde{\mathbf{s}} + \frac{4\mu}{a}h^2\left(\bar{\xi}\frac{\partial s_\alpha}{\partial\xi} + \eta\bar{\eta}h^2 s_\beta\right) \\
\tau_{\alpha\beta} &= \frac{2\mu}{a}\left[\bar{\xi}\frac{\partial}{\partial\xi}\left(hs_\beta\right) - \bar{\eta}\frac{\partial}{\partial\eta}\left(hs_\alpha\right)\right] \\
\tau_{\beta\beta} &= \lambda\nabla\cdot\tilde{\mathbf{s}} + \frac{4\mu}{a}h^2\left(-\bar{\eta}\frac{\partial s_\beta}{\partial\eta} + \xi\bar{\xi}h^2 s_\alpha\right)
\end{aligned}
\qquad \text{(A-7)}
$$

When the ϕ and χ functions from which $\tilde{\mathbf{s}}$ is obtained according to Eq. (3.3) are substituted into Eqs. (A-7), Eqs. (3.9) and (3.10) result.

APPENDIX B

ELASTIC PARAMETERS FOR SALT AND TUFF

Parameter	Salt*	Tuff**	
		Natural State	Natural State under Hydrostatic Pressure of 1000 psi
Y (psi)	1500	0.18×10^6	0.37×10^6
E (psi)	0.14×10^6	1200	5.00
σ	0.5	0.11	

*See Ref. 11.
**See Ref. 12, Table 6.

APPENDIX C

CALCULATION OF THE TRANSFORM OF THE IMPULSE FUNCTION

From Eqs. (5.6) and (5.14)

$$\vec{p}(\kappa, \omega) = A \int_0^\infty r dr J_0(\kappa r) \frac{e^{i\omega r/c}}{\left(a^2 + r^2\right)^2} \tag{C-1}$$

$$= -\frac{A}{2a} \frac{\partial}{\partial a} F(a) \tag{C-2}$$

where

$$F(a) \equiv \int_0^\infty r dr J_0(\kappa r) \frac{e^{i\omega r/c}}{a^2 + r^2} \tag{C-3}$$

Decomposing the integrand into even and odd functions,

$$F(a) = \frac{1}{2} \int_0^\infty \frac{r dr}{r^2 + a^2} J_0(\kappa r) \cos \frac{\omega}{c} r + i \frac{1}{2} \int_0^\infty \frac{r dr}{r^2 + a^2} J_0(\kappa r) \sin \frac{\omega}{c} r$$

$$= F_0(a) + i F_e(a)$$

The second of these integrals may be written

$$F_e(a) = \frac{1}{16i}\int_{-\infty}^{\infty} \frac{r\,dr}{r^2+a^2}\left[H_0^{(1)}(\kappa r)e^{i(\omega/c)r} + H_0^{(2)}(\kappa r)e^{i(\omega/c)r} - H_0^{(1)}(\kappa r)e^{-i(\omega/c)r} - H_0^{(2)}(\kappa r)e^{-i(\omega/c)r}\right]$$

and the integration carried out by closing the contour in the appropriate half plane. Since the only singularity in these four integrands is at the pole at $r = \pm ia$, the integrals are readily evaluated by applying the residue theorem. To obtain convergence for $K < \omega/c$, the upper half plane is used for the first two integrals and the lower half plane for the latter two. The situation is reversed for $K > \omega/c$. One obtains

$$F_e(a) = \begin{cases} \frac{\pi}{2} I_0(\kappa a)e^{-\omega a/c}, & \kappa < \omega/c \\ 0, & \kappa > \omega/c \end{cases} \qquad \text{(C-4)}$$

A similar calculation for $F_0(a)$, using only the first and fourth quadrants and noting that the integration down the positive imaginary axis cancels with one up the negative imaginary axis, yields

$$F_0(a) = \begin{cases} 0, & \kappa < \omega/c \\ \cosh \omega\frac{a}{c} K_0(\kappa a), & \kappa > \omega/c \end{cases} \qquad \text{(C-5)}$$

Since the subsequent evaluation of the integrand in Eq. (5.10) requires only a knowledge of $\bar{p}(\kappa, \omega)$ in the vicinity of the singularity at $K = k_R$ which is less than ω/c, only the upper expression in Eq. (C-4) is really of any interest. Inserting this result into Eq. (C-2) yields the result given in Eq. (5.15).

REFERENCES

1. W. M. Ewing, W. Jardetzky and F. Press, Elastic Waves in Layered Media, McGraw-Hill (1957).

2. A. Erdelyi (ed.), Bateman Manuscript Project, Tables of Integral Transforms, Vol. I, McGraw-Hill (1954) pp. 14 and 72.

3. H. A. Bethe, Theory of Seismic Decoupling, LA-2334. (Classified).

4. A. E. H. Love, Treatise on The Mathematical Theory of Elasticity, 4th Ed. Dover (1944) p. 250.

5. M. A. Sadowsky and E. Sternberg, J. Appl. Mech. 69, A-191 (1947).

6. I. S. Sokolnikoff, Mathematical Theory of Elasticity, 2nd Ed., McGraw-Hill (1956) p. 177

7. L. W. Mann, Los Alamos Code, T-5-2076.

8. J. Nuckolls, Livermore Report UOPDE 59-6, May 1959.

9. Stanford Research Institute, Operation Hardtack Project 26.1, Report ITR-1702, January, 1959, p. 6.

10. R. Hill, The Mathematical Theory of Plasticity, Oxford University Press (1956) p. 97 et seq.

11. S. Serata and E. F. Gloyna, Reactor Fuel Waste Disposal Project, Development of Design Principle for Disposal of Reactor Fuel Waste into Underground Salt Cavities, Report from the University of Texas, Department of Civil Engineering, Sanitary Engineering Research Laboratory, Austin, Texas. Work performed under contract AT (11-1)-490 with the Atomic Energy Commission, (1959).

12. G. W. Johnson, G. H. Higgins and C. E. Violet, J. Geophys. Res. 64, 1457 (1959).

13. L. M. Swift and D. C. Sachs, Air Pressure and Ground Shock Measurements, WT-711 January 1955. (Classified).

14. G. N. Watson, Treatise on the Theory of Bessel Functions, 2nd Ed., Cambridge University Press (1952) p. 388.

15. W. Magnus and F. Oberhettinger, Formulas and Theorems for the Special Functions of Mathematical Physics, Chelsea (1949) p. 66.